AN INTEGRATED STUDY OF TRIBOCORROSION IN A DUPLEX STAINLESS STEEL

A Thesis

by

ZHIHAO HUANG

Submitted to the Office of Graduate and Professional Studies of
Texas A&M University
in partial fulfillment of the requirements for the degree of

MASTER OF SCIENCE

Chair of Committee,	Hong Liang
Committee Members,	Partha Mukherjee
	Li Liu
Head of Department,	Andreas Polycarpou

December 2015

Major Subject: Mechanical Engineering

ABSTRACT

Tribocorrosion is one of the most dangerous threats to material systems due to the accelerated and uncontrollable damage. The interaction of mechanical rubbing and chemical corrosion causes material failure in a quite short time. Tribocorrosion widely exists in different industries, such as mining, oil and gas production, biomedical implants and chemical-mechanical planarization. This thesis studies the tribocorrosion in mild rubbing conditions. A new experimental approach was developed to study the effects of applied loads on passivation and surface defects. Results showed that properties of the passivation layer in duplex stainless steels were affected under different loads and surface defects elongated in the rubbing direction. This new experimental approach was proven to be an effective method to evaluate tribocorrosion in duplex stainless steels in mild wear conditions.

Primary experimental approaches were utilized in this study. A new methodology was developed by configuring an integrated triboelectrochemical tester. A flat-on-flat configuration was developed that contained a pair of flat rubbing parts, a tribometer and an electrochemical workstation. A duplex stainless steel 2205 was used due to the wide applications in corrosive environments. The tribocorrosion experiments were conducted in a 3.5wt% NaCl solution. The applied loads ranged from 1N to 3N at a fixed surface speed of 1.5cm/s. Analysis was carried out in evaluating the effects of mechanical rubbing on corrosion and passivation.

Results showed that mechanical rubbing promoted corrosion. Meanwhile, a passivation layer was generated due to the interaction of mechanical rubbing and corrosion. When the load was increased, the passivation current density increased first then decreased. The shapes and the sizes of surface defects were affected by different loads. The surface defects elongated in the rubbing direction. Detailed mechanisms were also discussed in this thesis.

This thesis includes six sections. After a brief introduction of tribocorrosion, the motivation and objectives of this study are discussed. A new integrated triboelectrochemical approach for studying tribocorrosion is discussed in section 3 along with materials and characterization. Section 4 discusses about the synergy of wear and passivation while the section 5 studies pitting during tribocorrosion. The dissertation ends with conclusion and recommended future work.

DEDICATION

This dissertation is dedicated to Dr. Hong Liang and my family.

ACKNOWLEDGEMENTS

I would like to thank my committee chair, Dr. Hong Liang, for her constant support in my academic career in Texas A&M University. This thesis would not have been possible without her help and guidance. I would also like to thank my committee members, Dr. Partha Mukherjee and Dr. Li Liu, for their guidance throughout this research.

Thanks also go to my friends, colleagues and the department faculty and staff for making my time at Texas A&M University a great experience. Specially thank Dr. Alex Fang for assistance in machining components for the experimental setup, Wei Dai in using the tribometer, and Huaping Xiao in using the electrochemical workstation. I would also like to thank STLE-Houston Session for providing me the scholarship in 2015, which encourages me in my research.

Finally, thanks to all my family for their love. Specially thank my parents for their support and encouragement, my uncle and aunt for their help and guidance, and my girlfriend for her patience.

NOMENCLATURE

CMP	Chemical-mechanical planarization
OCP	Open circuit potential
i	Current density
i_a	Anodic current density
i_c	Cathodic current density
E_0	Corrosion potential
E_p	Passivation potential
i_p	Passivation current density
MIC	Microbiological induced corrosion
CP	Cathodic protection

TABLE OF CONTENTS

Page

LIST OF FIGURES

LIST OF TABLES

1. INTRODUCTION

This section introduces some basics about corrosion. Focus will be on the costs and the electrochemical nature of corrosion, corrosion in stainless steels, and a brief background of tribocorrosion, including the principle and its state of the art.

1.1 Economic Impacts of Corrosion in the US

Corrosion is a gradual destruction of the chemical reaction between materials and their environments. The process is spontaneous and slow. However, corrosion costs much more than people expect. As shown in Figure 1-1, the costs of corrosion have been increasing rapidly in the past 15 years.

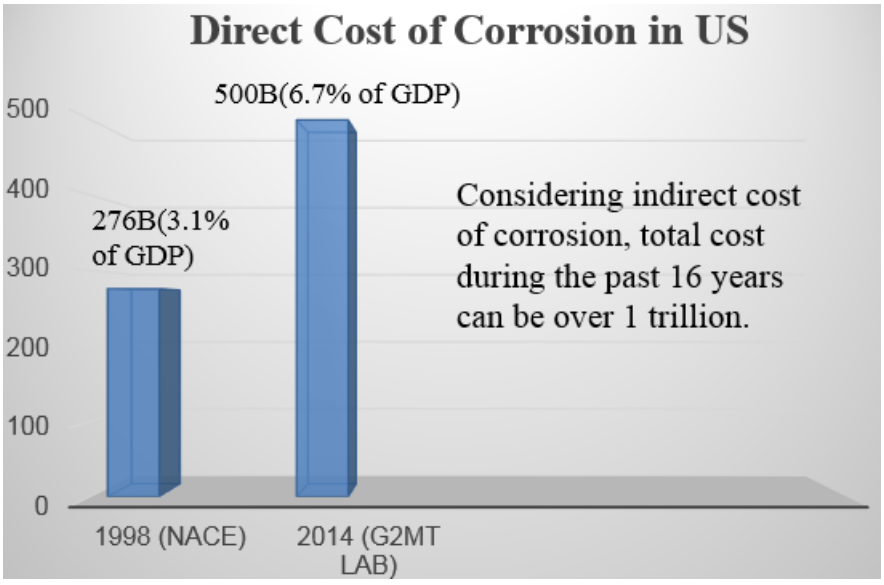

Figure 1-1 Costs of corrosion in the US.

In 1998, the National Association of Corrosion Engineers (NACE) reported that the total costs of corrosion in the US were estimated to be 276 billion, approximately 3.1% of Gross Domestic Product (GDP) [1]. In 2013, according to the latest report from the Generation 2 Material Technology (G2MT) lab, the direct costs of corrosion in the US have reached 500 billion, approximately 6.7% of GDP. Meanwhile, the indirect costs were estimated to be at least the same as the direct cost. This means that the total costs of corrosion would be over 1 trillion in 2013 [2]. In fact, corrosion has become one of the largest single expenses in the US economy.

Although it is impossible to completely prevent, corrosion can be controlled by some technical methods. Coating and cathodic protection (CP) are two main methods to control corrosion. They are sometimes applied together to provide a better protection than separately. For example, some offshore platforms are protected by coating with some corrosion resistant materials and then being connected with some sacrificial anodes. Because of the diversity of corrosion, coating and cathodic protection cannot provide a good protection all the time. Take the underground pipelines for example. If the coating material breaks down at some parts on the surface of the pipelines, the cathodic current will leak through the bare surface into soil and attract bacteria. Microbiological influenced corrosion (MIC) will take place once a certain amount of bacteria is accumulated [3, 4]. This will promote corrosion and cause failure of the pipelines in a short time. There exit a lot of similar cases. Industries are calling for more advanced methods to provide a better service in field. Mechanisms of different types of corrosion should be well studied to develop new protective technologies.

1.2 Electrochemistry in Corrosion

The nature of corrosion is electrochemical reaction. Corrosion processes by transferring electrons from the anode to the cathode. Corrosion will take place when two materials with different potentials (an anode and a cathode respectively) are connected and immersed in a conductive electrolyte. Consider the reactions between zinc (Zn) and copper (Cu) in the sulfuric acid (H_2SO_4), as shown in Figure 1-2:

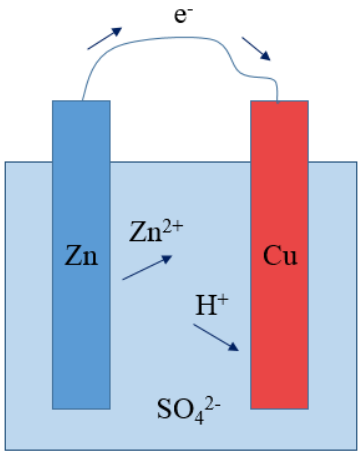

Figure 1-2 Reaction between zinc and copper in the sulfuric acid.

Reactions are taking place as the following equations:

$$Zn \rightarrow Zn^{2+} + 2e^{-}$$

$$2H^{+} + 2e^{-} \rightarrow H_2$$

Zinc (Zn, anode) reacts with the sulfuric acid (H_2SO_4) and loses electrons. Meanwhile, hydrogen ions (H^+) gain electrons and form bubbles on the surface of copper

(Cu, cathode). Finally, zinc (Zn) will corrode. In these spontaneous reactions, zinc (Zn), copper (Cu) and sulfuric acid (H_2SO_4) is the anode, the cathode and the electrolyte respectively.

The electrochemical approach was discovered to be an enabling method in corrosion protection by scientists in the late 70's and early 80's. The electrochemical approach can be used in the in-situ monitoring of the corrosion study in labs. Potential and current can be measured from the continuously transferring electrons in the corrosion process of a certain material. The corrosion behavior can be obtained by analyzing the potential and current. The potential indicates the activity of the material and the current indicates the corrosion rate.

A number of experimental methods for electrochemical testing have been standardized by the National Association of Corrosion Engineers (NACE) and the American Society of Testing Material (ASTM) [5]. Some standards are listed in Table 1-1.

Table 1-1 Standard electrochemical measurements in corrosion tests [6-12].

Designation	*Title*
ASTM G59-97	Standard Test Method for Conducting Potentiodynamic Polarization Resistance Measurements
ASTM G61-86	Standard Test Method for Conducting Cyclic Potentiodynamic Polarization Resistance Measurements for Localized Corrosion
ASTM G61-12	Standard Test Method for Measurements of Corrosion Potentials of Aluminum Alloy
ASTM G71-81	Standard Guide for Conducting and Evaluating Galvanic Corrosion Tests in Electrolyte
ASTM G82-98	Standard Guide for Development and Use of a Galvanic Series for Predicting Galvanic Corrosion Performance
ASTM G100-89	Standard Test Method for Conducting Cyclic Galvanostaircase Polarization
ASTM 150-13	Standard Test Method for Electrochemical Critical Pitting Temperature Testing of Stainless Steel

The open circuit potential (OCP) experiments and the polarization experiments are two main methods to study corrosion in lab. In an open circuit potential (OCP) experiment, as shown in Figure 1-3, the corrosion potential (E_{corr}) is recorded as a function of time (t). The open circuit potential reaches a stable value (E_s), as shown in

Figure 1-3, means that the corrosion system is stable at that moment. The open circuit potential test is necessary before any electrochemical corrosion experiment.

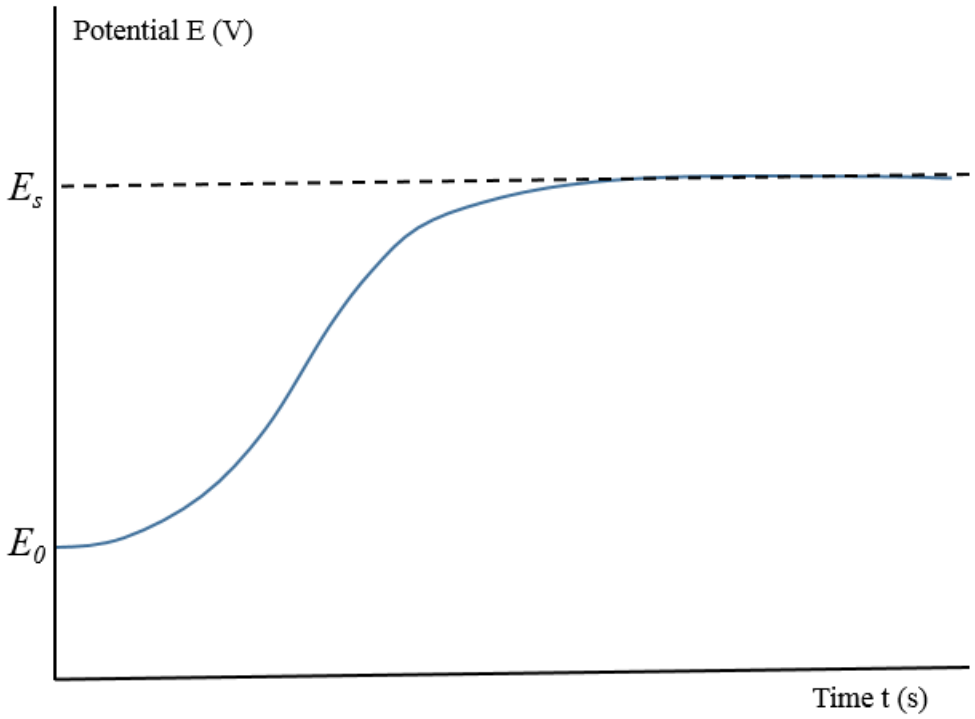

Figure 1-3 The open circuit potential experiment.

The polarization experiment can determine the corrosion current density, which can be used to calculate the corrosion rate. In a corrosion reaction, the total current is a sum of the anodic and the cathodic current. As shown in Figure 1-4, the blue dash line represents the current density of an anodic reaction and the black dash line represents the current density of a cathodic reaction. Meanwhile, the blue-half curve and the black-half curve represent the total current density. The blue-half curve is the anodic part and the

black-half curve is the cathodic part. When corrosion takes place at a potential of E_0, which is defined as the equilibrium state, the blue dash line crosses the black dash line with a value of i_0 in the current density. This indicates that the rate of the anodic reaction equals the rate of the cathodic reaction. Therefore, the total current density in an equilibrium state is zero. As shown in Figure 1-4, when the blue-half curve and the black-half curve meet at the purple dash line, the total current density is zero. However, the anodic current density indicates the corrosion rate of the anode and it cannot be measured directly at the potential of E_0. The polarization experiment is a method to obtain the anodic current density at potential of E_0.

In a polarization experiment, an external potential is applied on the electrode to force the reaction away from the equilibrium state. If a positive potential, which is E_a in Figure 1-4, is applied on the test sample, the reaction will enter the anodic state, which is the blue-half curve. A green dash line, which is parallel to the X axis, is drawn from E_a cross the black and the blue dash lines. The cross point of the green and the black dash lines indicates a value of i_c in the cathodic current density. The cross point of the green and the blue dash lines indicates a value of i_a in the anodic current density. Compared with the current density at the potential of E_0, the anodic current density is much higher than the cathodic current density at the potential of E_a. This indicates that a positive potential promotes the anodic reaction and decreases the cathodic reaction. Because the cathodic current density is very limited, the total current density can be calculated as the anodic current density at the potential of E_a. The opposite situations exist when a cathodic potential is applied. Therefore, the total current density at an anodic or a

cathodic potential can be obtained in this way, which can consist the blue-half and the black-half curves. When the blue-half and the black-half curves are obtained, the cross point of the blue and the black dash lines can be determined by a linear fitting. The value in the X axis of this cross point is the current density at the potential of E_0. Conducting the linear fitting in a polarization curve is called Tafel fitting [13].

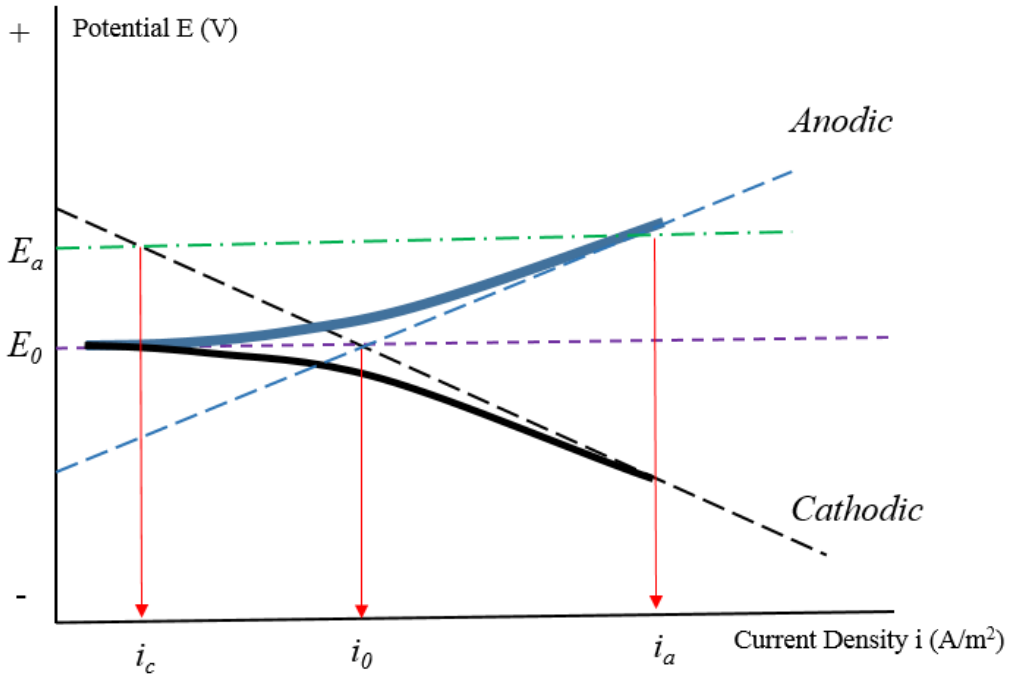

Figure 1-4 The illustration of the Tafel fitting.

The polarization experiment can also determine the corrosion behavior of a certain material. In the plot of a complete polarization curve, as shown in Figure 1-5, the Y axis is the applied potential and the X axis is the responded current density from the

test sample. This plot indicates the different corrosion activities of a certain material with different potentials. A polarization curve usually includes four regions, which is the cathodic protected region, the active corrosion region, the passive region and the transpassive region.

In the cathodic protected region, which is indicated from *a* to *b* in Figure 1-5, a cathodic current is applied on the test sample. The test sample will gain electrons from the power source. Therefore, no corrosion takes place on the test sample in this region.

When a positive potential ($E > E_0$) is applied, the test sample enters the active corrosion region (from *b* to *c* in Figure 1-5) first. In the active corrosion region, the test sample will lose electrons at a high rate. Therefore, the responded current density from the test sample will increase quickly as the applied potential increases. This indicates that the surface of the test sample is very active and corrosion takes place at a high rate.

When the positive potential increases and reaches a critical potential, which is shown as E_p (point *c*) in Figure 1-5, the responded current density from the test sample will decrease. This critical potential is defined as the passivation potential. Theoretically, the decreased current density will reach a stable value as the applied potential increases, which is shown as i_{pass} in Figure 1-5. This stable current density is defined as the passivation current density. The potential region, which ranges from *c* to *d*, is defined as the passive region.

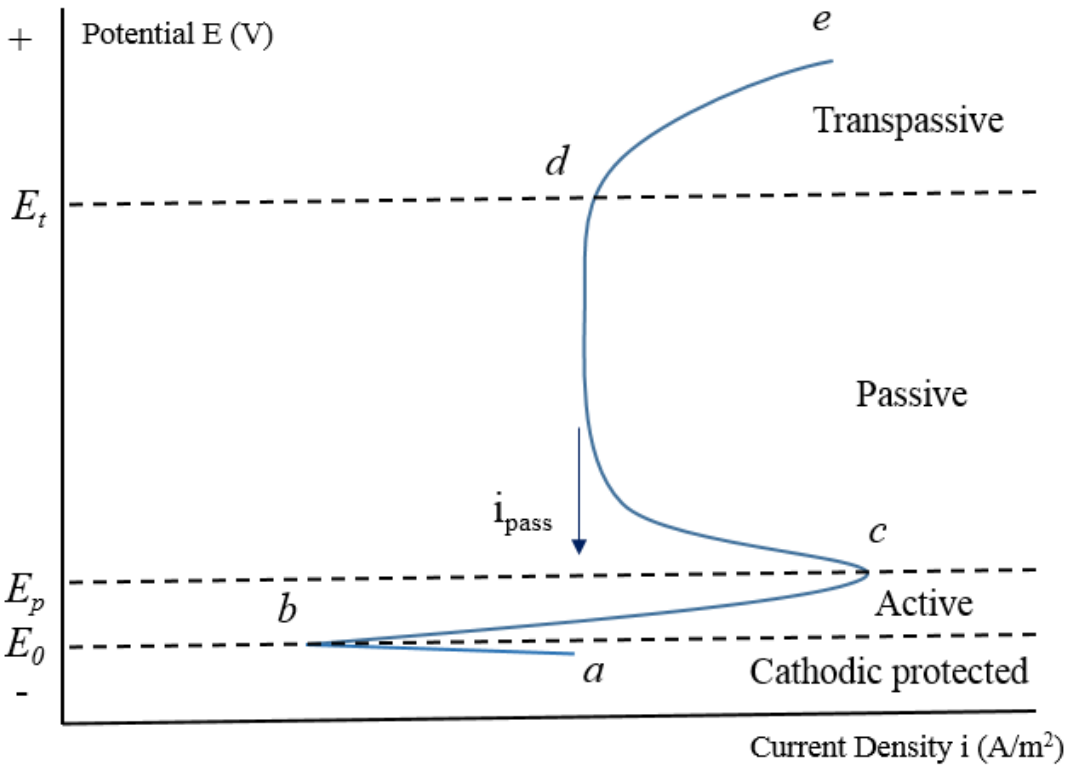

Figure 1-5 The illustration of the polarization curve.

In the passive region, a passivation layer will build on the surface of the test sample. Take the stainless steel as an example. The passivation layer is of a crucial importance to maintain the stainless steel to be corrosion resistant in a harsh environment. The passivation layer is thin but tight and it will be built on the surface when the stainless steel is exposed to an environment with enough oxygen. The passivation layer acts like a barrier to prevent oxygen accessing the internal material, which can slow down corrosion taking place. In a polarization experiment, the corrosion is promoted by the applied positive potential. Therefore, a passivation layer will build on the surface of the test sample when the passivation potential is reached. The responded

current density from the test sample decreases because that the passivation layer slows corrosion down.

When the applied potential increases over the other critical potential (E_t), which is defined as the transpassive potential, the responded current density will not maintain at a low level any more. The current density will increase as the applied potential increases. The region, which is indicated from *d* to *e* in Figure 1-5, is defined as the transpassive region. In the transpassive region, the passivation layer is not stable any more. Under the high applied potential, it will react with the electrolyte and finally break down. Lacking of the protection of the passivation layer, corrosion will be active again. Therefore, the current density will increase again in a polarization curve.

1.3 Basic Principles of Tribocorrosion

There are reported at least nine types of corrosion in the world, such as the uniform corrosion, galvanic corrosion, pitting corrosion, crevice corrosion, environmentally-induced cracking, hydrogen damage, intergranular corrosion, dealloying, erosion and tribocorrosion.

Compared with the first eight types of corrosion listed above, tribocorrosion is less understood. The word “tribocorrosion” is combined with two parts, which are tribology and corrosion. According to the ASTM standard, tribocorrosion is a synergetic action of the chemical corrosion and the mechanical wear which leads more significant interaction than separately [14]. Before this term came up, many other phrases had been used to describe the interacted phenomena, such as erosion-corrosion, wear accelerated

corrosion, corrosive wear and fretting corrosion. The general mechanisms of tribocorrosion are as follows. If two materials are rubbing with each other in a corrosive environment, the mechanical wear will change the surface property and affect the corrosion behavior. Meanwhile, the altered corrosion will affect the wear process. As shown in Figure 1-6 [15], the process of tribocorrosion in an active-passive material is as follows. The mechanical wear affects the passivation layer on the surface and promotes corrosion. Meanwhile, the corrosion makes the surface rougher, which provides a more severe condition for the mechanical wear. Finally, the interaction of two aspects causes a large amount of material loss [16-18]. Because of this complex process, the detailed mechanisms of the tribocorrosion process are still unclear.

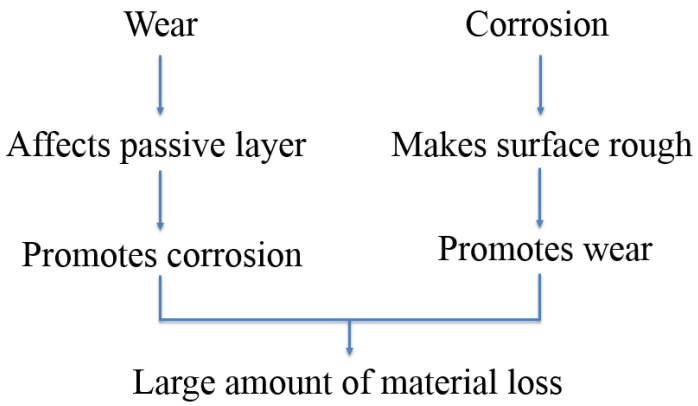

Figure 1-6 The process of tribocorrosion.

However, tribocorrosion is also believed to take place in the mild wear conditions, in which the mechanical rubbing is gentle and will not destroy the

passivation layer. The passivation in tribocorrosion in the mild wear conditions is believed as a dynamic process, which includes the depassivation and repassivation. The energy difference between the depassivation and repassivation determines the growth and property of the passivation layer.

1.4 Roles of Tribocorrosion in Industry

Tribocorrosion widely exists in several industries, such like mining industry, drilling process, petrochemical refining, oil and gas production, biomedical implants, military equipment and others. In mining and drilling industry, the drill bits cut rocks in the environment containing the soil and the drilling fluids. In the offshore oil and gas production, many pieces of equipment work in the splash area with a high oxygen concentration. For biomedical implants, the hip joints fail under the interaction of abrasion and corrosion in human bodies. In addition, the silicon discs can be polished to the high surface quality using a chemical and mechanical planarization (CMP) method, which mechanisms are also tribocorrosion.

A study of the failure in the piston rods of the riser tensioners was presented at the NACE international conference in 2009 [19]. In this study, the failed piston rods, which substrates were covered with different coating materials, were investigated and analyzed. Results showed that most of the piston rods failed in a relatively short service time. The riser tensioning system is used on an offshore platform to compensate the movement of the sea surface and provide a perpendicular tension for the drilling riser. The riser tensioner will corrode easily in the splash environment, which contains enough

oxygen and water. The worst situation is that once the wear particles, such as sands, enter the lubrication and sealing box, severe abrasion and corrosion will take place together. The surface coating layer will crack and delaminate into pieces with sharp edges. When these delaminated coating materials enter the sealing box, the shape edges will destroy o-ring or other sealing components, which will cause loss of the tension power. Finally, the whole system will break down. When severe cracks or other damages on the surface coating layer are observed, the piston rod of the riser tensioner has to be replaced before any accident taking place. This study showed that every investigated piston rod of the riser tensioner was designed with a 3-5 years of service life. However, most of the piston rods failed in 1 year. Some of them even failed in a service time less than 3 months. Such short service life will cause a very high production cost in offshore oil and gas. The similar situations widely exist in other pieces of equipment in offshore and subsea oil and gas production. As discussed above, for real life applications, new materials and more effective protection methods are needed to ensure a long service life for manufacturing equipment.

1.5 The Research State of Tribocorrosion

The research of tribocorrosion can be traced back to the ancient time when the study of tribology began. Hertz and Reynolds developed the mathematical formalisms for the contact mechanics and the hydrodynamic lubrication at the beginning of 20th century [20]. In order to improve the design of the lubrication and tribological components, an integration of mechanical, material, chemistry and physics was proposed

by a British government committee in the early 1960s. This brought scientists and engineers from different fields together to start the new researches in tribocorrosion. Since the late 1970s, several different mechanisms about synergy of electrochemical and mechanical damage have been reported. Tribocorrosion related words, such as tribochemical wear, oxidation wear, corrosive wear and wear-corrosion, were used in literature during 1970s to early 1990s. The term "tribocorrosion" has been adopted in the sliding system and the mechanism has been studied since 1990s [21].

In the past 10 years, an extraordinary growth has taken place in the field of tribocorrosion. A tribocorrosion research network has been established to link engineers and scientists together in 2000. This organization is based in the University of Strathclyde. It is led by Dr. Margaret Stack. Tribocorrosion research is mainly conducted in Europe, North America and Asia. The research groups in different regions focus on different aspects and applications in tribocorrosion. For example, Dr. Mischler's group (EPFL, Switzerland) studies the mechanical and electrochemical deterioration mechanism in the tribocorrosion [16, 22, 23]. Pro. Johnsen's group (NTNU, Norway) focuses on the multi-degradation mechanisms and modeling of tribocorrosion under the static and cyclic loads [17, 24]. Pro. Dearnley's group (University of Southampton, UK) studies the erosion-corrosion interaction for the marine and offshore applications [25]. Dr. Liang's group (Texas A&M University, USA) studies the chemical mechanical planarization (CMP) method and post-CMP cleaning process [26-33].

After several years of development, many achievements have been obtained. According to different purposes, many combinations of materials and electrolytes were

chosen in the tribocorrosion experiments. The experiment applications included the fundamental study, the biochemical application, the coating selection and others. For example, UNS S30403, S31603 and S32760 stainless steels were chosen to study the synergistic effects of abrasion and corrosion by J.O.Bello for a fundamental study [34]. High carbon and low carbon Co–Cr–Mo alloys were used to study the tribocorrosion behavior for the biomedical implants by Yu Yan [35]. Plasma nitride Ti-6Al-4V alloy was investigated in the neutral NaCl solution for the surface treatment study [36]. Combined corrosion-wear degradation of Ni–SiC nanostructured composite was studied for the coating material selection by L. Benea [37].

In the prior study, the experiment geometric model is dominated by the ball-on-disc configuration, as shown in Figure 1-7. The test samples were rubbed against a sphere counterpart. Potential, current and corrosion resistance were measured during the tribocorrosion experiments.

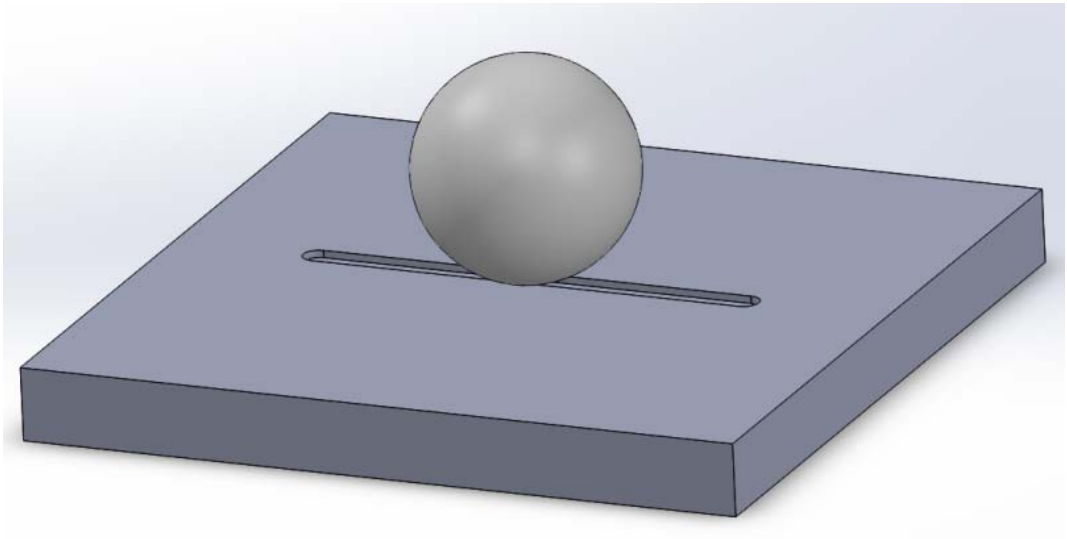

Figure 1-7 A ball-on-disc configuration.

For example, a tribocorrosion experiment was carried out by Takadoum in 1996 [38]. In this experiment, an iron plate was rubbed against a vertically mounted alumina ball pin in the sulfuric acid with a reciprocating motion. Results showed that obvious wear tracks and the deformation of substrate took place. The observed crystallographic etching area indicated that the passivation layer was destroyed and the active corrosion in that region.

Four main data-analysis approaches were established, including the synergistic approach, the mechanistic approach, the third body approach and the nanochemical wear approach. The synergistic approach is the most well established and most widely accepted method to analyze the data of the tribocorrosion experiment. The ASTM G119 standard was established on this theoretical approach.

The synergistic approach is used to evaluate the interaction between abrasion and corrosion for a sliding system in an active-passive material. The synergistic approach was first proposed by a group in the US Bureau of Mines between mid-1980s and early 1990s. The equations and parameters are listed below [14].

$$T = W_0 + C_0 + S$$

$$S = \Delta C_w + \Delta W_0$$

$$\text{Total synergism factor} = T / (T - S)$$

$$\text{Corrosion augmentation factor} = (C_0 + \Delta C_w) / C_0$$

$$\text{Wear augmentation factor} = (W_0 + \Delta W_c) / W_0$$

T is total tribocorrosion rate; W_0 is pure mechanical wear rate; C_0 is pure chemical corrosion rate; S is synergistic factor; ΔC_w is wear accelerated corrosion; ΔW_c is corrosion accelerated wear. The procedures of this approach are as followed:

1. Measure T in a tribocorrosion test by mass lost method
2. Determine C_0 in a corrosion test by Faraday's Law
3. Measure W_0 in a wear test with cathodic protection by mass lost method
4. Determine C_w in a tribocorrosion test by Faraday's Law
5. Calculate ΔC_w by subtracting C_0 from C_w
6. Determine other parameters by equations above

1.6 Limitation in Current Research and Standards

Although many valuable achievements have been obtained, a lot of limitations still exist in the previous research and standards. The limitations mainly exist in three aspects, including the experiment approach, the experiment technology and equipment and the data analysis approach.

1.6.1 Limitation in the previous experiment approach

As mentioned in section 1.5, tribocorrosion study is dominated by the ball-on-disc model. This experiment approach has two main limitations: the aggressive wear condition and the effect of the galvanic reaction.

1. Aggressive wear condition

In the ball-on-disc configuration, high loads are applied on the limited contact surface area. The high contact pressure is always reached, which will cause the

deformation in the surface and subsurface material. For example, a small ball pin with 1cm diameter can provide up to 768 MPa contact pressure under 10N load. If load is increased to 20N, the contact pressure can reach 967MPa [24]. When such high contact pressure exceeds the yield strength of the test sample, the plastic deformation will take place. For the active-passive materials, the passivation layer cannot be remained under such aggressive wear conditions. However, tribocorrosion is also believed to take place in mild wear conditions, such like in the interface of the piston rod and sealing parts. The abrasion effect on corrosion in the active-passive materials cannot be studied using the ball-on-disc approach.

2. The effect of the galvanic reaction

In the experiments using the ball-on-disc configuration, the severe wear tracks were reported [23, 39, 40]. As shown in Figure 1-8, a passivation layer will build on the surface when an active-passive material is exposed to the corrosive environment with enough oxygen. In the tribocorrosion process, this passivation layer will be removed and hard to regenerate. Once wear track is formed under both wear and corrosion, bare material will expose to the corrosive environment. As shown in Figure 1-8, the potential of the material in the wear track is negative, which indicates that the material is active. Meanwhile, the potential of the material is the passivation region is positive, which means that the materials is noble. A galvanic cell will build between the wear track and the passivation region because of this potential difference. The material in the wear track is the anode and that in the passivation region is the cathode. The galvanic reaction has great effect on the corrosion. The accelerated corrosion will take place in the material in

the wear track, which may cause more severe tribocorrosion in that region. Some research groups are studying the galvanic coupling effect in tribocorrosion [24].

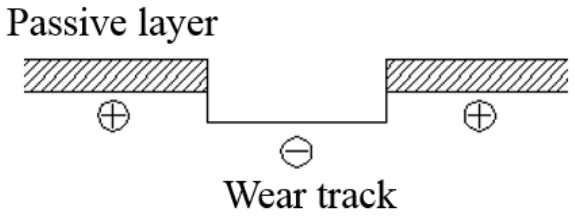

Figure 1-8 The illustration of the galvanic effect.

1.6.2 Limitation in the current technology and equipment

Limitations in the current technology and equipment are mainly in three aspects.

1. Limitation in the experimental approach

Although a number of in-situ experiments are reported, no experiment approach provides an in-situ method to monitor the deformation in the interface in the tribocorrosion process. The in-situ experiment of corrosion can be conducted using the electrochemical approach. The in-situ experiment of wear can be conducted by recording the surface roughness. If scientists want to check the surface morphology in the tribocorrosion process, the only method is to compare the graphs before and after experiments. There is no effective way to conduct an in-situ experiment under present technology, which can monitor the growth of a surface defect in the tribocorrosion process.

2. Limitation in the understanding of the interface reaction

The real interface reaction in the tribocorrosion process is still unclear. Reaction for a pure metal in different combinations of PH and potential can be tracked in the Pourbaix Diagrams. Many other parameters affect the chemical reactions, such as temperature, pressure and so on. Therefore, it is very complicated to determine the real chemical reaction in the interface in an engineering material. When the tribocorrosion takes place, wear and corrosion will affect each other. Lacking of information about the real interface reaction, the detailed mechanisms of tribocorrosion cannot be reached.

1.6.3 Limitation in the current standards

As mentioned in section 1.5, the ASTM G119, "Standard Guide for Determining Synergism between Wear and Corrosion", is the mainly accepted standard to evaluate tribocorrosion behavior in an active-passive material. This guide is to calculate the increased material loss rate and to provide attribution of wear and corrosion in the synergism. This approach can only be applied in tribocorrosion experiment in the liquid and slurry. It cannot be used in the environment of gas or solid. For the metallic tribocorrosion experiments, this standard cannot be used in the systems where corrosion products, such as the oxidation layer, will be remained on the surface after tribocorrosion. As discussed, if the passivation layer generates in the tribocorrosion process, the ASTM G119 is no longer useful.

2. MOTIVATION AND OBJECTIVES

As discussed in section 1, corrosion has become one of the largest expenses in the US economy. Tribocorrosion plays the most important roles in the degradation in most engineering applications where mechanical forces and chemical attack the materials together. Tribocorrosion is one of the most challenging in the field of corrosion, which always causes severe damage to materials in a quite short time. However, understanding tribocorrosion is still limited due to its synergetic aspects and complicated mechanisms. This research aims to generate fundamental understanding in tribocorrosion. The focus will be on duplex stainless steels. The reason is that tribocorrosion widely exists in offshore oil & gas production. Duplex stainless steel is a commonly used material in harsh environments because of its excellent mechanical properties and corrosion resistance. Studying tribocorrosion in this material will benefit its application in energy exploration and that in marine environment.

There are three major objectives to be achieved in this research.

1. Develop an effective approach to study tribocorrosion in mild wear conditions.

As discussed in section 1, a lot of work has been done to study tribocorrosion in the past 20 years. However, most of them were carried out in very aggressive wear conditions by using a ball-on-disc configuration. It is impossible to study the effect of mechanical rubbing on the passivation behavior in tribocorrosion using this approach. An alternative approach is needed to study tribocorrosion in mild wear conditions. The

mild wear condition is necessary because it promotes pinpointing mechanical against chemical interactions.

2. Identify key parameters to understand the effects of mechanical rubbing on corrosion.

Tribocorrosion is the interaction of mechanical wear and chemical corrosion. Key parameters need to be identified in order to understand their effects. We will evaluate the experimental tribocorrosion parameters such as applied force, sliding speed, environment temperature and contact area.

3. Obtain fundamental understanding of tribocorrosion in mild wear conditions.

Prior studies have been focused on aggressive wear conditions where plastic deformation took place under a high contact pressure. In this research, we will investigate the corrosion and passivation under various mechanical energies. The surface conditions, such as physical (morphology) and chemical (passivation and/or pitting), will be evaluated. Basic understanding is expected to generate.

To succeed, experimental approaches will be used. It includes design and configuration of a tribo-electrochemical tester and surface characterization techniques. Detailed experimental plans will be discussed in section 3.

3. EXPERIMENT PROCEDURES

This section discusses about the approach, materials and experiment procedures implanted in the present research. First, a new integrated triboelectrochemical approach is discussed in section 3.1. Second, the materials and setups in this approach are described in sections 3.2 and 3.3. Third, the test parameters and surface characterization are discussed in details in sections 3.4 and 3.5. Finally, some important issues are presented in section 3.6.

3.1 A New Integrated Triboelectrochemical Approach

In this study, a new integrated triboelectrochemical approach was developed to study corrosion that is influenced by wear. An experimental setup was designed and configured that includes a pair of flat rubbing parts, a tribometer and an electrochemical workstation. As shown in Figure 3-1, a square test sample with a large surface area was designated for this study. At the same time, a deformable material with a larger surface area was selected as the counterpart. The counterpart was adhered to the bottom of a large container. A sufficient amount of electrolyte of 500ml was kept in the container during the tribocorrosion process to minimize the effect of change in PH. As shown in Figure 3-2, the pair of rubbing parts, the tribometer and the electrochemical workstation were connected to conduct tribocorrosion tests. A linear reciprocating motion was selected. The surface speed and the rubbing distance were fixed at a low value. Applied loads ranged from 1N to 3N. The rubbing distance was selected to be 3 cm.

There are several advantages of this new approach.

1. No plastic deformation will take place in the test sample

The area of the contact surface between the test sample and the counterpart is considered larger than that in the previous studies. Under the low load, the contact pressure on the surface of the test sample is much lower than the yield strength. Therefore, there is no plastic deformation taking place on the surface of duplex stainless steel sample.

2. Elimination of galvanic effects

The surface area of the counterpart is larger than that of the test sample. This makes sure that the mechanical wear will be applied uniformly on the surface of the test sample during the tribocorrosion process. No galvanic cell can be built in this condition. The effect of the galvanic reaction will be avoided.

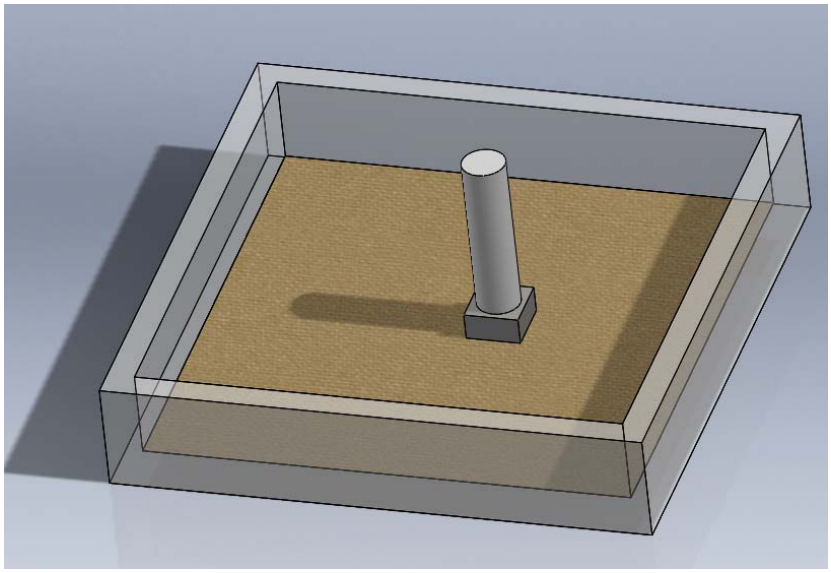

Figure 3-1 A flat-on-flat test configuration.

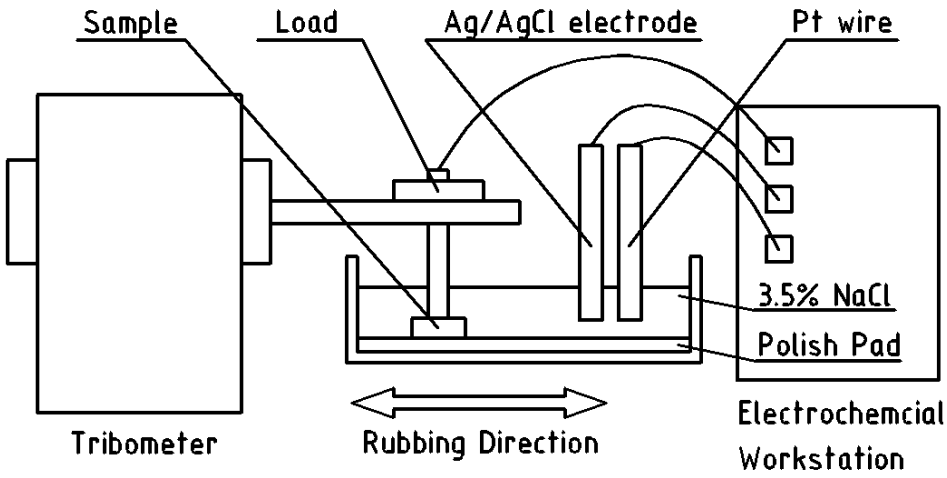

Figure 3-2 Illustration of a new configuration for tribocorrosion experiments. It contains a pair of flat rubbing parts, a tribometer and an electrochemical workstation. The test sample rubs against the counterpart in a linear reciprocating motion.

3.2 Materials and Sample Preparation

3.2.1 Materials

Duplex stainless steel 2205 was chosen as the test material for this tribocorrosion study. Its superior properties, such as high strength, high resistance to pitting corrosion, cracking and stress corrosion, low coefficient to thermal expansion, are desirable for engineering applications that endure harsh environments. Its applications include heat exchangers, tubes and pipes for production of oil and gas exploration, mechanical and structure component in chloride contained environment, utility and industrial system exposed to high corrosion fatigue. It has 50wt% ferrite and 50wt% austenite in the microstructure. Its chemical composition is shown in Table 3-1 (McMaster Carr).

Table 3-1 Chemical composition of duplex stainless steel [41].

Element	*Weight per cent (%)*
Fe	Balanced
N	0.14-0.20
P	0-0.03
Cr	22-23
Ni	4.5-6.5
C	0-0.030
Mn	0-2.00
Mo	3.0-3.5
Si	0-1.00
S	0-0.020

A soft polishing pad was used as the counterpart. This pad, as known as Politex polish pad, is a composite of urethane and polyester. This polish pad will not induce any severe scratch to the test sample of duplex stainless steel.

3.2.2 Sample Preparation

As described above, a square test sample of the duplex stainless steel 2205 was selected in this study. The test sample was prepared using the following procedures as Figure 3-3. Figure 3-3 was drawn using Solidworks to briefly show the process of manufacturing a test sample.

1. Cut the test sample into small pieces

First, the plate sample of duplex stainless steel 2205 was cut into small square pieces with a 1.1cm x 1.1cm surface area using a band saw. Second, the small sample was grinded using a #120 sand paper. The length of each side in a test sample was $1\ cm \pm 1\ mm$.

2. Mounted the test sample on a sample holder

First, a nonconductive rod with the high stiffness and the suitable diameter was chosen as the sample holder. A PVC tube with a diameter of 0.8 cm was selected in this study. Second, a small hole was drilled near one top using a bench drill. Third, the oxidation layer and contamination on the raw surface was cleaned by polishing with a #120 sand paper. Finally, the test sample was mounted on the sample holder with a super glue.

3. Adhered a copper wire to the test sample

First, a copper wire was put into the sample holder and a conductive glue was filled through the hole. Second, the test sample was kept for at least 24 hours to let the conductive glue become strong. Finally, the conductivity between the copper wire and the test sample was checked with a multimeter.

4. Polished the test surface

First, the non-test surfaces were covered with nail oil. Second, the non-tested surfaces were covered with the water proof adhesive tape after 24 hours. Third, the test surface was polished with the #240, #400 and #800 sand papers and then the diamond

polishing paste. Finally, the conductivity between the copper wire and the test sample was checked with a multimeter.

5. Cleaned and sealed the test surface for the tribocorrosion tests

First, the test surface was cleaned with distilled water and then acetone. Second, the test surface was sealed away from the oxygen with a clean paper towel. Finally, the test sample was kept in the vacuum cage.

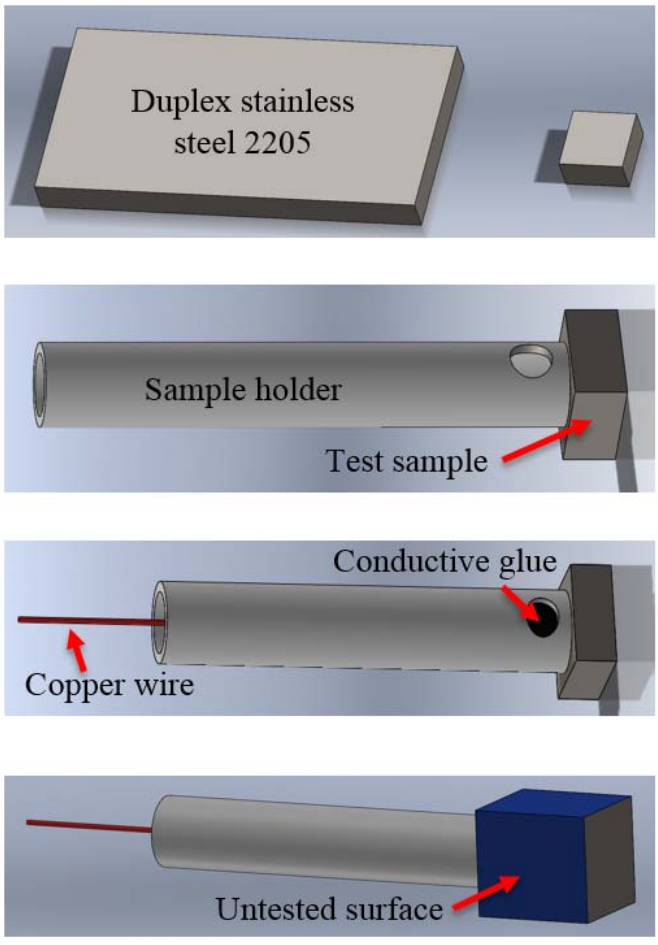

Figure 3-3 Sample preparation.

3.3 Setups

In this study, three main pieces of equipment were used to conduct the tribocorrosion tests and the surface characterization: a tribometer, an electrochemical workstation with a three-electrode system and an interferometer. The setup is shown in Figure 3-2. The linear rubbing motion was provided and controlled by a CSM tribometer. An electrochemical workstation, Gamry Reference 600, and a three-electrode system were connected to conduct corrosion tests, collecting potential and current. In this three-electrode system, working electrode (WE) was the test sample, duplex stainless steel 2205. The reference electrode (RE) was a standard Ag/AgCl/saturated KCl electrode, which is suitable for the sodium chloride (NaCl) electrolyte. The counter electrode (CE) was a platinum wire. All of these pieces of equipment were assembled as shown in Figure 3-2.

3.4 Experimental Conditions

In this tribocorrosion study, open circuit potential (OCP) tests, potentiodynamic and potentiostatic polarization tests were conducted in a linear rubbing motion. Parameters of tribology and corrosion test are shown in Table 3-2 and Table 3-3.

Table 3-2 Tribology Test Parameters.

Load	0,1,2,3N
Speed	0.5cm/s (max)
Distance	3cm
Contact Area	$1cm^2$
Temperature	75°F

Table 3-3 Corrosion Test Parameters.

Potential (vs V_{ref})	Potentiodynamic: -0.2V-1.2V Potentiostatic: 0.8V
Scanning Rate	2mV/s
Sample Period	Potentiodynamic: 700s Potentiostatic: 600s
Conditioning Time	60s

3.5 Surface Characterization

Surface characterization was carried out using an interferometer (Zygo) after the tribocorrosion test. The procedures were as follows.

First, the test sample was taken off from the plastic holder. The test surface was cleaned with distilled water and then acetone. Second, the interferometer was connected with the compressed air supply. The pressure of the compressed air was adjusted to 80 psi. Third, the position of the test sample in the interferometer was adjusted until fringes

showed up. The position of the test sample was adjusted again until only two fringes existed. Finally, the surface could be observed and measured. 3D models and cross section plots of the surfaces were obtained.

3.6 Factors To Be Considered

The electrochemical corrosion test is very sensitive to detailed conditions. Even temperature change in the lab will affect the reaction rate, shifting the test curve abnormally. Therefore, it is necessary to pay attention to every single aspect. Some important issues are listed as follows.

1. Calibrate the electrochemical workstation (Gamry Reference 600) carefully

Two steps should be taken carefully. Firstly, seal the dummy cell in a faraday cage to block the outer electromagnetic field. And the faraday cage must be connected with the ground to keep the same potential inside. Secondly, select the correct frequency of the inlet current according to the AC power source. In the Garmy software setup procedures, two different current frequencies are provided. Make sure the correct one is selected.

2. Keep the working electrolyte saturated all the time

The reference potential is provided by the reference electrode, which is the Ag/AgCl electrode is this study. The potential of the reference electrode is determined by the concentration of the working electrolyte inside. The working electrolyte can be a saturated NaCl, a saturated KCl or a saturated $NaSO_4$. The working electrolyte should be selected according to the testing electrolyte. In this study, the test electrolyte and the

working electrolyte were chosen to be a 3.5 wt% NaCl solution and a saturated KCl solution respectively. During the tribocorrosion tests, the KCl will disperse from the working electrolyte to the test electrolyte spontaneously. Therefore, it is very important to keep the KCl solution in the reference electrode saturated after tests. And excess crystallized KCl should be kept in the saturated solution after tests. Before the first test, the reference electrode is recommended to be kept in the saturated KCl solution for at least 24 hours.

3. Choose a right reference electrode according to the test environment

Take the Ag/AgCl reference electrode as an example. It cannot be used in a very alkaline condition. The hydroxide ion (OH^-) will oxide the silver which will block ions exchanging in the electrode. The best test environment for an Ag/AgCl reference electrode is the one with a PH value from 3 to 8.

4. Prepare enough test electrolyte before test

The electrochemical corrosion test is very sensitive to conditions. Even difference in the test electrolyte will cause an obvious error. The concentration of test solution will affect the corrosion rate. Making at least 1 liter of a 3.5wt% NaCl solution in a long neck flask at once is recommended.

5. Choose a suitable material as the sample holder

An insulated and rigid material should be selected for the sample holder. The diameter of holder tube also should be selected carefully to fit the arm of tribometer. If the tube is too thin, vibration will take place in the rubbing process that will cause a lot of noises.

6. Select a suitable potential scanning rate

A suitable scanning rate should be selected. A slow scanning rate provides more information in a certain potential range. It is suitable in a lot of corrosion tests. However, it will bring in a lot of noises in a tribocorrosion test. That is because the surface property of a test sample is unstable. If a fast scanning rate is selected, some important points cannot be collected successfully. So, before conducting tribocorrosion tests, a suitable scanning rate should be selected according to the test conditions.

3.7 Conclusions

This section discussed about the procedures and experimental details of the thesis research. As seen, an innovative approach was developed and implied to this research. Using the integrated approach of tribology and corrosion, we expect to reveal the mechanisms of tribocorrosion. Sections 4 and 5 discuss about the discovery and principles behind it.

4 FRICTION-INDUCED PASSIVATION

This section discusses about the passivation phenomena in a tribocorrosion process. Tribocorrosion experiments were conducted using the new approach that has been discussed in section 3. The potentiodynamic and potentiostatic polarization experiments were conducted under different loads in order to study the role of applied loads. Results showed that the mechanical rubbing promotes the formation of a passivation layer, instead of removing the material. The generation of a passivation layer in the tribocorrosion process is discussed in section 4.1. The growth of a passivation layer is discussed in section 4.2. Finally, in section 4.3, the possible mechanisms are discussed.

4.1 Generation of A Passivation Layer

The potentiodynamic polarization experiments were conducted to study the active-passive tribocorrosion in a duplex stainless steel. The experiments were conducted under the load ranging from 0N to 3N. The potentiodynamic polarization curves are shown in Figure 4-1 and Figure 4-2. In these polarization curves, the Y axis represents the applied potential E (V) and the X axis represents the responded current density i (uA/cm^2) from the test samples.

The green curve was obtained as a reference in the corrosion test without mechanical rubbing. In this curve, four corrosion regions can be determined, which are divided by the small triangles in the Figure 4-1. The cathodic protected region ranges

from -0.2V to -0.17V. Active corrosion takes place from -0.17V to -0.1V. Passivation region is from -0.1V to 0.8V. Above 0.8V is the transpassive region. Meanwhile, sudden increase in current density can be observed at several points in the passive region. Pitting is believed to take place at these points. In the forming process of pitting, the passive layer will be partly destroyed, which causes sudden increases in current density. The pitting potential can be defined as the potential as soon as the currently density increases. In the green curve, the pitting potential is around 0.2V.

The other curves were obtained in tribocorrosion experiments. The experiments were repeated for three times. The error bars indicated the variations of the current density in the experiments. The black curve was obtained under a load of 1N. As shown in Figure 4-1, compared with the green curve, the black curve shows up at the right side. This phenomenon indicates that the current density increases in all corrosion regions under mechanical rubbing. Meanwhile, the slope of the black curve in the passive region is bigger than that of the green curve. Compared to the active corrosion region, the passivation current density does not increase as much as the potential increases. This means that a passivation layer was formed in the tribocorrosion process that slows down corrosion taking place.

The blue curve was obtained under a load of 2N. As shown in Figure 4-2, compared with the green curve, the blue curve also shows up at the high current density direction. Increase in the current density can also be found in all corrosion regions. This means that mechanical rubbing under a high load can promote corrosion on the sample surface. Meanwhile, the slope of the blue curve in the passivation region is larger than

that of the green curve. This means that the passivation layer can be formed under mechanical rubbing even under a high load. However, the passivation current density in the blue curve is larger than that in the black curve, which may indicate that less surface area is covered by the passivation layer during the tribocorrosion process.

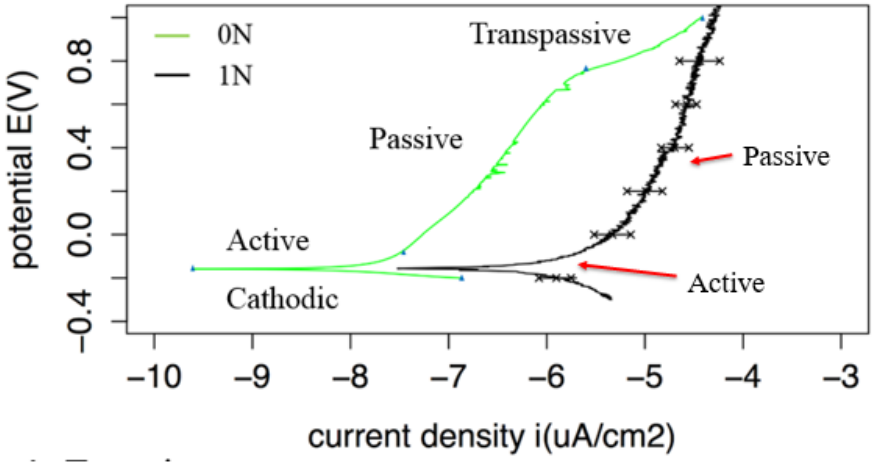

Figure 4-1 Potentiodynamic polarization curve (a).

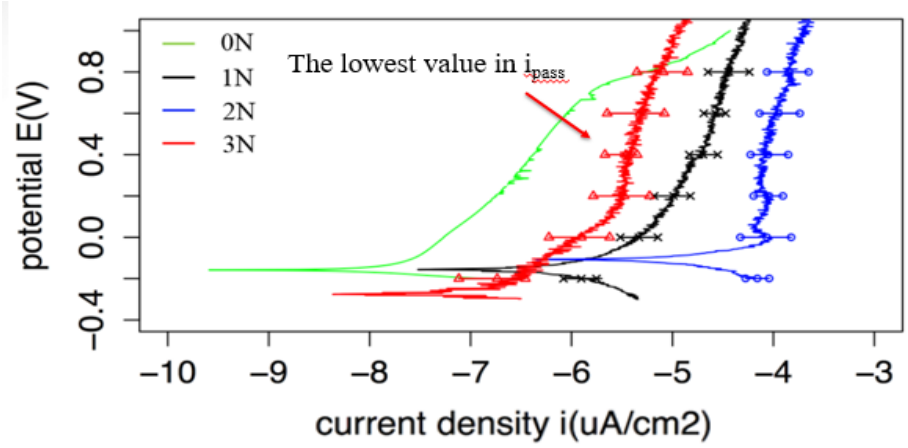

Figure 4-2 Potentiodynamic polarization curve (b).

The red curve was obtained under a load of 3N. As shown in Figure 4-2, it appears between the green (0N) and black (1N) curves. It indicates that mechanical rubbing under a load of 3N can also promote corrosion. Meanwhile, the slope of the red curve in the passivation region is larger than that of the green curve. This means that the passivation layer can be formed even under the highest load selected in this study. However, when the load was increased from 1N to 2N, the passivation current density increased. When the load was increased from 2N to 3N, the passivation current density decreased. This phenomenon is very interesting. It indicates that the property of the passivation layer, which was formed under the load of 3N, has been changed a lot. Possible reasons are discussed in the section 4.3. The lowest value in the passivation current density may indicate that the passivation layer may cover the most surface area.

4.2 Growth of A Passivation Layer

As discussed in section 4.1, a passivation layer was observed to form in the tribocorrosion process. The potentiostatic polarization tests were conducted to study the growth of a passive layer under loads ranging from 1N to 3N. The potentiostatic polarization curves are shown as Figure 4-3. In these curves, the X axis represents the test time t (s) and the Y axis represents the responded current I (A) from the test samples. These experiments were repeated for three times and error bars indicate the variations of the current in the experiments.

The black curve was obtained under a load of 1N. In this curve, the current increases to a stable value at a high rate. This whole curve can be divided into three

regions. The first region is from 0s to 200s. The current increases quickly in this region. The rate in the current is 7.75mA/s. This indicates that the surface of the test sample is active. In the other word, the passivation layer has covered little surface area on the test sample. The second region starts at 200s and ends at 300s. In this region, the current increases at a lower rate than that in the first region. The rate of the current is 3mA/s. This indicates that the surface of the test sample is more stable than that in the first region. In the other word, the passivation layer has covered more surface area on the test sample. The third region is from 300s to 600s. In this region, the current does not change a lot. The rate in the current is 0.5mA/s. This indicates that the surface of the test sample is stable. The passivation layer has covered a certain surface area on the test sample.

The blue curve was obtained under a load of 2N. This curve can be divided into three regions. The first region is from 0s to 300s. In the first region, the current increases at a high rate. The rate of the current is 6.7mA/s. As discussed above, the surface of the test sample is active in this region and the passivation layer has covered little surface area on the test sample. The second region is from 300s to 450s. In the second region, the current increases at a lower rate than that in the first region. The rate of the current is 4mA/s. This indicates the surface is more stable than that in the first region and the passivation layer has covered more surface area on the test sample. The third region is from 450s to 600s. In this region, the current does not change a lot. The rate of the current is 0.67mA/s. The current oscillates severely in the third region. It indicates that the passivation layer is generated and destroyed simultaneously. More detailed mechanisms are discussed in section 4.3.

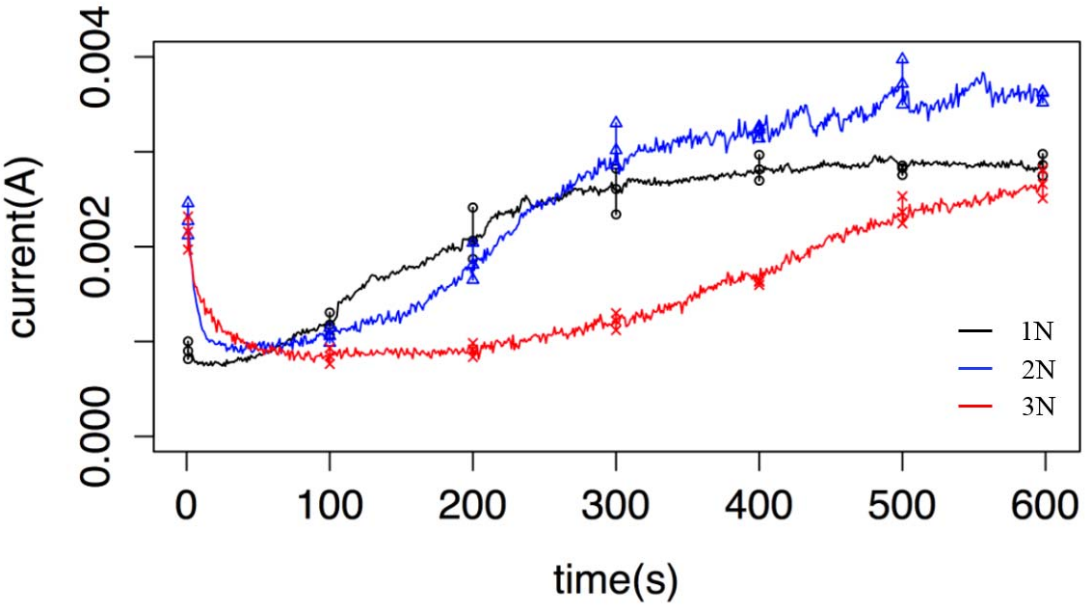

Figure 4-3 Potentiostatic polarization curve.

The red curve was obtained under a load of 3N. The current increases at a constantly low rate. Therefore, only one region can be defined in the red curve. The increasing rate of the current is 2.5mA/s. This indicates that the surface of the test sample is stable in the tribocorrosion process. The passivation layer has covered a certain surface area on the test sample. In addition, the current does not oscillate severely in the red curve. More detailed mechanism is discussed in section 4.3.

4.3 Proposed Mechanisms

As discussed in sections 4.1 and 4.2, the potentiodynamic and potentiostatic polarization experiments were conducted to study tribocorrosion in a duplex stainless steel 2205. A passivation layer is observed to remain in tribocorrosion process in mild wear conditions. Meanwhile, mechanical rubbing under different loads affected the property and the generation process of a passivation layer. Possible mechanisms for the promoted corrosion, the generation and the growth of a passivation layer are discussed as follows:

1. Accelerated corrosion

Compared with the corrosion experiment, mechanical rubbing was observed to promote corrosion in the tribocorrosion experiments. Corrosion is an electrochemical reaction. In this study, a positive potential was applied on the sample of the duplex stainless steel 2205. The duplex stainless steel 2205 corroded and released electrons into the NaCl solution. Meanwhile, the hydrogen ions gained electrons at the surface of the platinum wire. The main reactions are as follows:

Anodic reactions:

$$Fe - 3e^- \longrightarrow Fe^{3+}$$

$$Ni - 2e^- \longrightarrow Ni^{2+}$$

$$Cr - 3e^- \longrightarrow Cr^{3+}$$

Cathodic reaction:

$$2H^+ + 2e^- \longrightarrow H_2$$

In the aqueous corrosion experiment without mechanical rubbing (the green curve in section 4.1), an electrical double layer is built between the corroding metal and the bulk of aqueous environment in the equilibrium state. As shown in Figure 4-4 and Figure 4-5, a positive potential (+V) is applied on the electrode (the gray part). This applied potential causes an electrical field near the surface of the corroding metal. The water molecules of the solution will align themselves in this electrical field. There are two models for the electrical double layer. In the Helmholtz's model, as shown in Figure 4-4, a layer with a thickness of one molecule is "adhered" to the surface of the electrode. In the Gouy-Chapman's model [42], as shown in Figure 4-5, a number of counter ions will be attracted to the surface of the electrode. However, these ions are tend to diffuse into the liquid phase near the surface of the electrode until a counter potential is set up to restrict their movements.

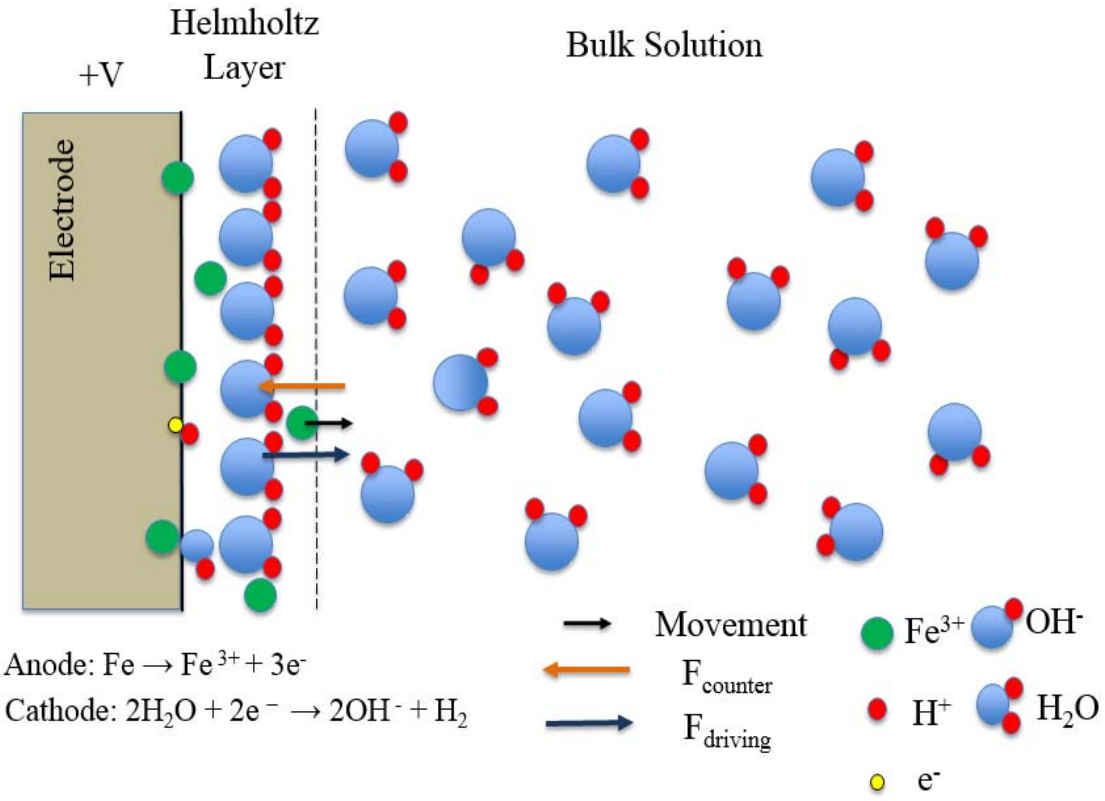

Figure 4-4 The Helmholtz model of an electrical double layer in a corrosion reaction.

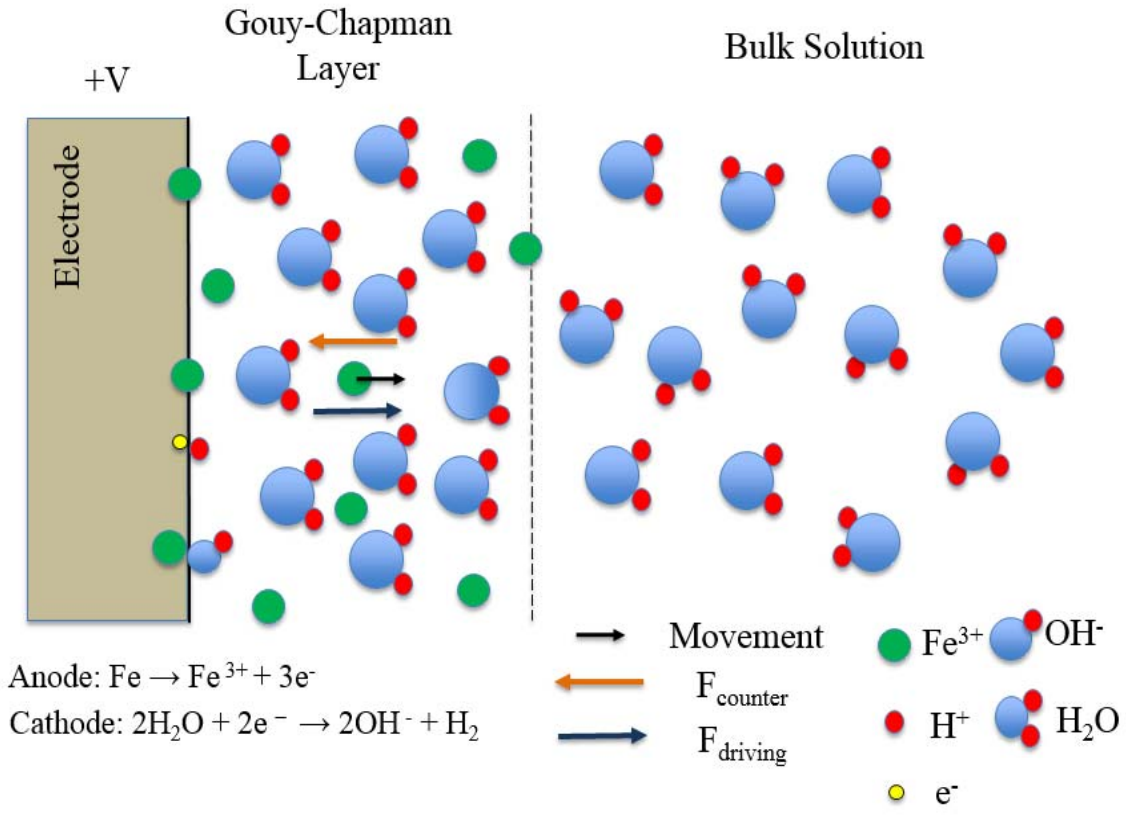

Figure 4-5 The Gouy-Chapman model of an electrical double layer in a corrosion reaction.

When corrosion takes place, a metallic ion must go through the electrical double layer and enter the bulk of free electrolyte. This electrical double layer is like a potential barrier to the metallic ions, which kinetically affects the corrosion rate. As shown in Figure 4-4 and Figure 4-5, the green dots represent the metallic ions that are released from the metal (the duplex stainless steel 2205 in this study). Two forces will act on the metallic ion (the green dot) when it goes through the electrical double layer (the movement is shown as the black arrow). One is the driving force (the blue arrow), which

is generated by the applied potential, and the other is the counter force (the orange arrow) which is generated by the electrical double layer.

In the tribocorrosion experiments, mechanical rubbing under different loads was applied on the surface of the test sample (the electrode). As shown in Figure 4-6, no electrical double is believed to build near the surface of the electrode. Therefore, only the driving force (the blue arrow) will be applied on the metallic ion (the green dot) when the metallic ion is released from the metal and enters the bulk electrolyte. Compared with that in the corrosion experiment, the metallic ion enters the bulk electrolyte with less potential resistance in the tribocorrosion experiments. This indicates that corrosion rate in the tribocorrosion experiments will be higher than that in the corrosion experiments.

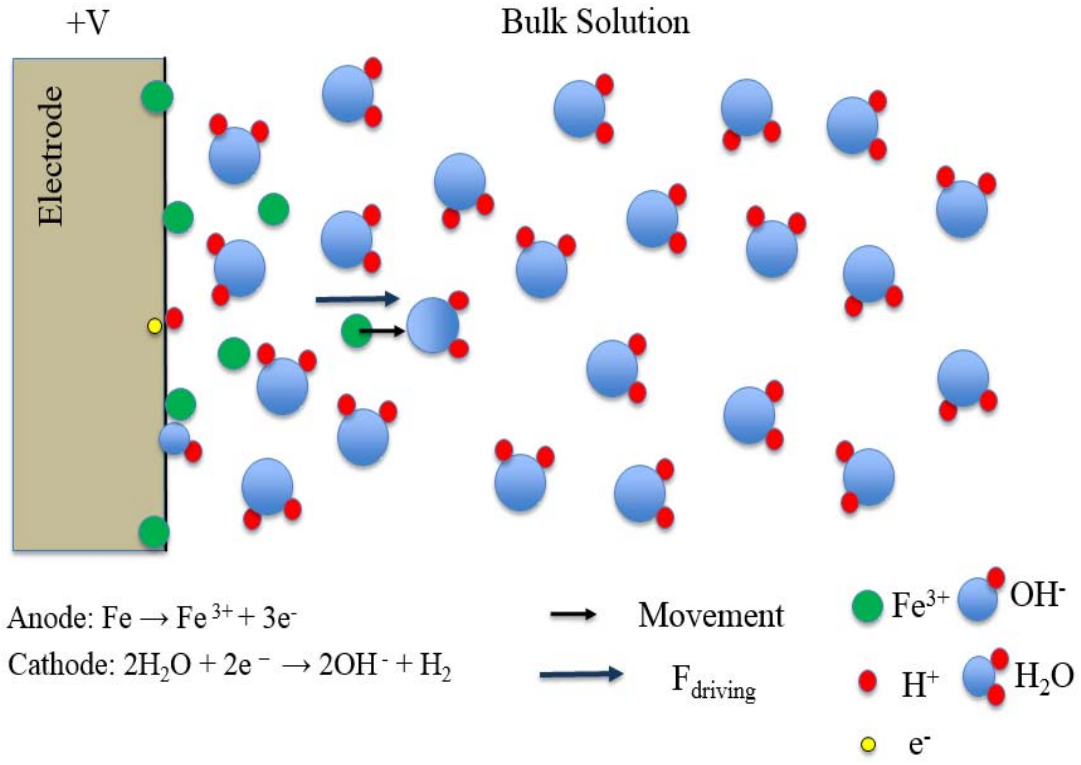

Figure 4-6 No electrical double layer is built in a tribocorrosion reaction.

2. The generation of a passivation layer

A passivation layer was observed to generate in the tribocorrosion experiments. Passivation in the tribocorrosion process is dynamic, including the depassivation and repassivation. Details in the depassivation and repassivation will be discussed in the next part in this section.

Reasons for the generation of the passivation layer are discussed in following three aspects. First, a low-contact pressure was applied in this study. The area of the test samples is 1 cm^2. The applied loads ranged from 1N to 3N. Therefore, the highest

contact pressure was $3x10^4$ Pa. The yield strength of the duplex stainless steel is estimated as 448 MPa. The contact pressure in this study was much lower than the yield strength of a duplex stainless steel 2205. No plastic deformation took place in the tribocorrosion process. Second, a deformable counterpart, which is a Politex polish pad, was used in this study. This polish pad is a composite of urethane and polyester. It is softer than the duplex stainless steel and it will not induce severe scratches on the surface of the test samples. Such mild wear conditions provided a good environment for the generation of a passivation layer. At the same time, as shown in Figure 4-7, this soft polish pad was observed to deform under a load. The higher the load that was applied, the more deformation took place, which provided more contact surface area. Because of the increased contact area and load, more heat was generated during the rubbing motion. Corrosion was kinetically accelerated to form a passivation layer. The third reason is the high chromium content in the duplex stainless steel 2205. Its chromium content is approximately 22-23% by mass. Chromium can be quickly oxidized to form chromium dioxide, which is the main content of a passivation layer. All these three aspects are thought to be responsible for the generation of a passivation layer in tribocorrosion under mild wear conditions.

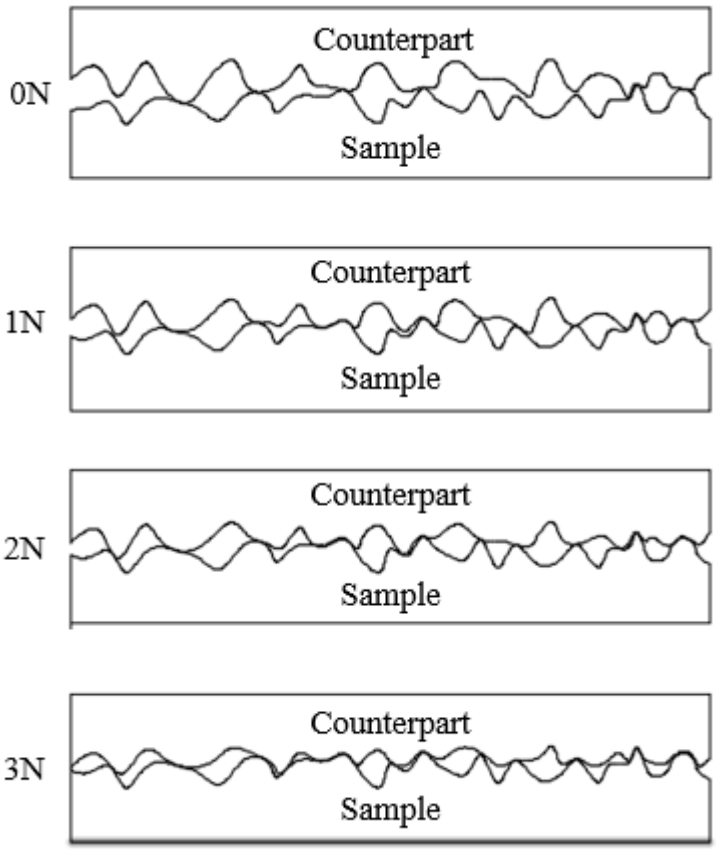

Figure 4-7 Contact surface under different loads.

3. Passivation

As discussed in the sections 4.1 and 4.2, mechanical rubbing under different loads affected the passivation behavior. When the mechanical rubbing under the highest load (3N) was applied, the passivation current density was the lowest in the potentiodynamic polarization experiments and the responded current from the test sample increased at a lowest rate. According to these observed phenomena, a question

can be asked: does mechanical rubbing under a high load generate more material loss in the passivation layer?

Consider the sliding abrasion model (Equation 4-1):

$$V = K_{ab} * W * L/H$$

Equation 4-1 The Archard model in the sliding abrasion [20].

V is material remove rate; K_{ab} is a constant; W is applied load; L is wear distance; H is the hardness of test sample.

If only the effect of mechanical rubbing is considered, mechanical rubbing under a high load will definitely generate more material loss. Because the wear distance (L) and hardness (H) were fixed in this study. However, the passivation current density decreased under the highest applied load, which does not match this expected tendency.

Passivation is believed as a dynamic process in tribocorrosion. The passivation layer will be removed and regenerated by the interaction of mechanical rubbing and corrosion simultaneously. Here is a simply model of passivation in a tribocorrosion process, as shown in Equation 4-2:

$$\text{Tribocorrosion} = \text{Depassivation} + \text{Repassivation}$$

Equation 4-2 Passivation in tribocorrosion.

If the energy of the mechanical wear is much higher than that of the corrosion, the depassivation will dominate the whole process. The passive layer will be damaged slowly and destroyed finally. If the energy of the corrosion is higher than that of the mechanical wear, the repassivation will be stronger than the depassivation. The passivation layer will be able to generate in the tribocorrosion process.

At this stage, the detailed mechanisms about the growth and the reduction of the passivation layer are not clear. The proposed relationship between repassivation and depassivation is illustrated in Figure 4-8. In this study, a passivation layer was always found to generate during the tribocorrosion process. This indicates that the repassivation is always stronger than the depassivation. When the applied loads changed, the repassivation and the depassivation changed in different amount respectively. When the loads increased from 1N to 2N, the increased amount in the repassivation is less than that in the depassivation under mechanical rubbing. When the loads increased from 2N to 3N, the increased amount in the repassivation is more than that in the depassivation under mechanical rubbing.

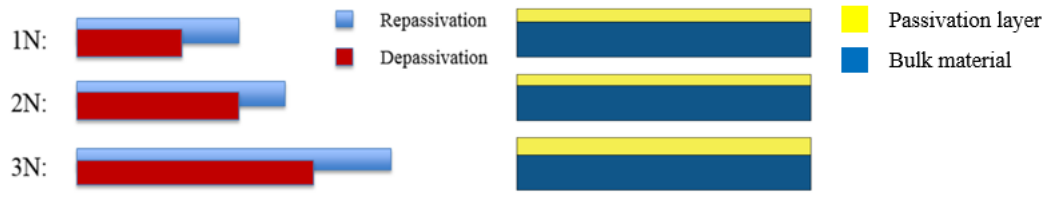

Figure 4-8 Relationship between depassivation and repassivation under different loads.

4.4 Conclusions

This section discussed about the passivation in the tribocorrosion in the mild-wear conditions. As discussed in sections 4.1 and 4.2, a passivation layer was observed to generate and mechanical rubbing under different loads affected the passivation in the tribocorrosion process. Possible mechanisms are discussed in the section 4.3.

5 PITTING IN TRIBOCORROSION

This section discusses about the pitting formed in the tribocorrosion process. Surface characterization was conducted using an interferometer after the potentiodynamic polarization experiments. Results showed that mechanical rubbing through various loads affected the shapes and sizes of surface pits. Detailed discussions and proposed mechanisms are discussed in section 5.1. Conclusion is discussed in section 5.2.

5.1 Transformation of Pits

Surface characterization was conducted using an interferometer after the potentiodynamic polarization experiments. Through the surface profile, the geometries of pitting on the surface and in the subsurface were measurable using this technique. The size and morphology of pits, before and after tribocorrosion, were compared. Results are shown as follows.

1. Reference surface

After polishing, the surface of test samples was observed in the interferometer as a reference. Results are shown in Figure 5-1. The Figure 5-1 (a) is the topography of the test sample. Red represents that the area is at a high altitude and blue at a low altitude. The colorful scale bar on the right in Figure 5-1 (a) indicates the height range of this plot, which is from -0.03654 um to 0.04569 um. The Figure 5-1 (b) is a profile of the

cross-section. In the Figure 5-1 (b), the X axis represents the area which is indicated as a line between two triangles in the Figure 5-1 (a). The Y axis represents the height of each point on the X axis. As shown in Figure 5-1 (a) and Figure 5-1 (b), the polished surface is flat.

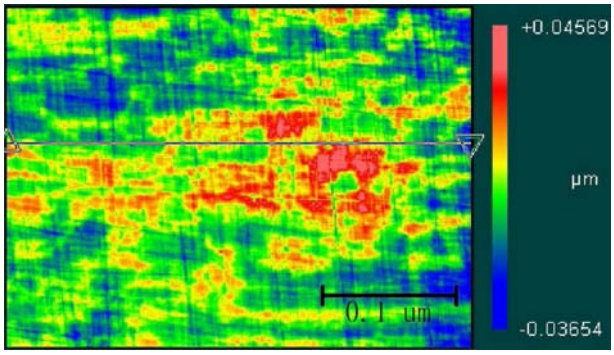

Figure 5-1 (a) Topography of surface after polishing.

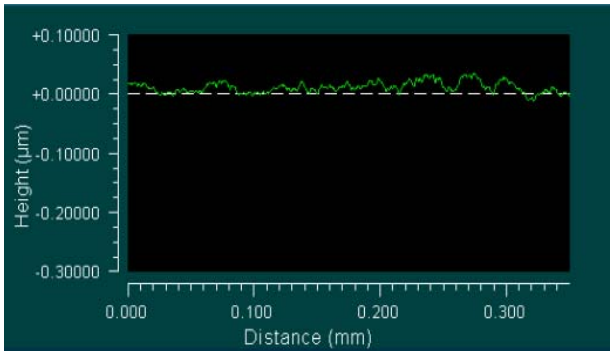

Figure 5-1 (b) Profile of cross section after polishing.

2. Corroded surface

The sample surface after the potentiodynamic experiment without mechanical rubbing is shown in Figure 5-2 and Figure 5-3. Figure 5-2 (a) and Figure 5-3 (a) are the topographies of the sample surface. Figure 5-2 (b) and Figure 5-3 (b) are the profiles of

the cross-section. As shown in Figure 5-2 (a) and Figure 5-3 (a), a number of small pits appear on the sample surface. The pits are round with an average diameter of 0.0214 mm. As shown in Figure 5-2 (b) and Figure 5-3 (b), the pits are very deep compared with their diameters on the surface. As discussed in the section 4.1 of the section 4, pitting was observed in the potentiodynamic polarization experiment without applying mechanical rubbing (the sudden increases in the current density in the green curve). Therefore, the small pit is pitting.

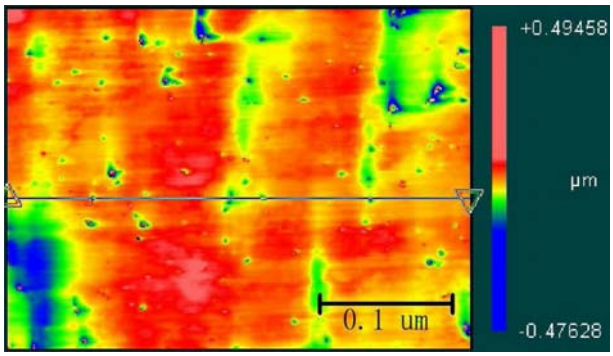

Figure 5-2 (a) Topography of surface at pit A after corrosion.

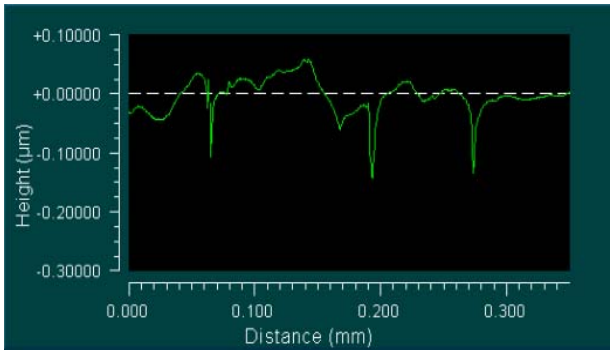

Figure 5-2 (b) Profile of cross section at pit A after corrosion.

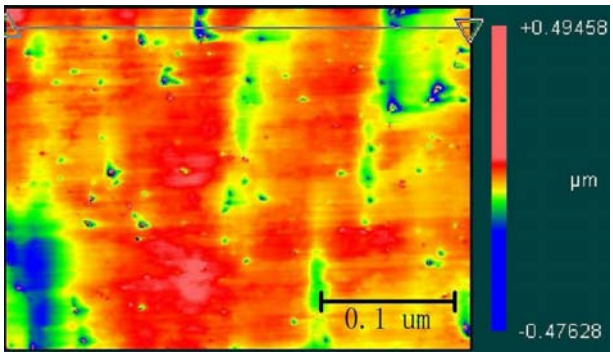

Figure 5-3 (a) Topography of surface at pit B after corrosion.

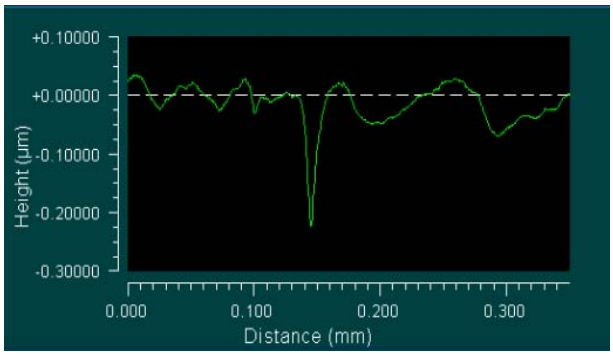

Figure 5-3 (b) Profile of cross section at pit B after corrosion.

3. Tribocorroded surface

The sample surfaces after the potentiodynamic polarization experiments with mechanical rubbing are shown in Figures from 5-4 to 5-9. The defects on each surface are observed in two directions, i.e., in the rubbing direction and in that perpendicular to the rubbing direction. Surfaces after tribocorrosion under mechanical rubbing with a load of 1N are shown in Figure 5-4 and Figure 5-5. Pitting-like surface defects appeared under a load of 1N. Topographies of the sample surface are shown in Figure 5-4 (a) and Figure 5-5 (a). Profiles of the cross-section are shown in Figure 5-4 (b) and Figure 5-5

(b). The red-yellow stripes in Figure 5-4 (a) and Figure 5-5 (a) are the wear tracks induced by mechanical rubbing. As mentioned in the section 3.1 of section 3, a linear reciprocating motion was used in this study. Therefore, these wear tracks indicate the direction of rubbing. The sizes of the pits in the rubbing direction are almost same as the sizes in that perpendicular to the rubbing direction. However, compared with that in the Figure 5-2 and Figure 5-3, these pits maintain in the round shapes with an average diameter of 0.0458 mm.

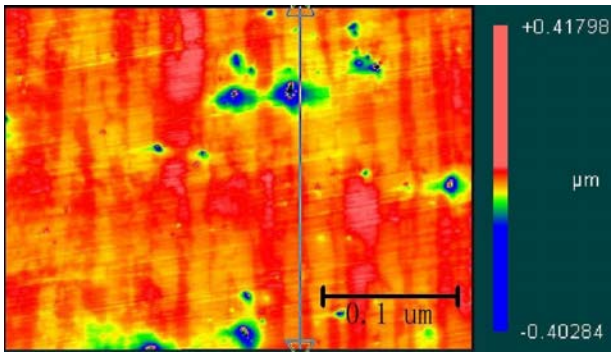

Figure 5-4 (a) Topography of surface after tribocorrosion (1N, in the rubbing direction).

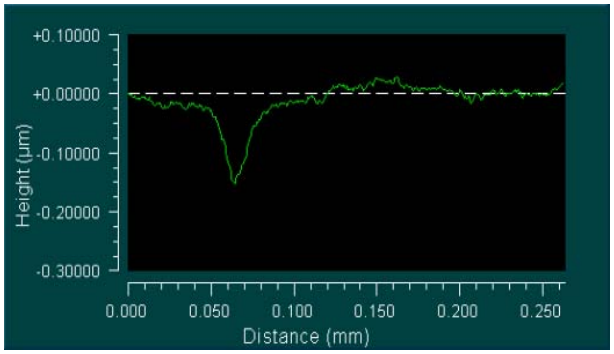

Figure 5-4 (b) Profile of cross section after tribocorrosion (1N, in the rubbing direction).

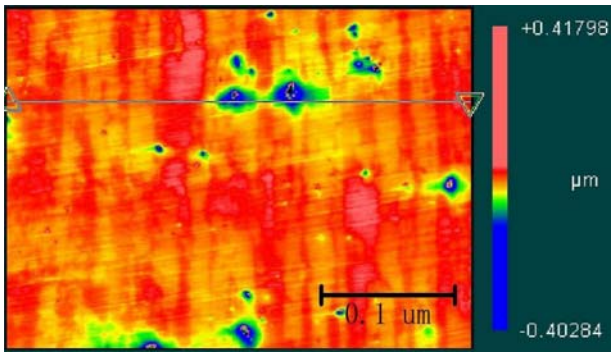

Figure 5-5 (a) Topography of surface after tribocorrosion (1N, perpendicular to the rubbing direction).

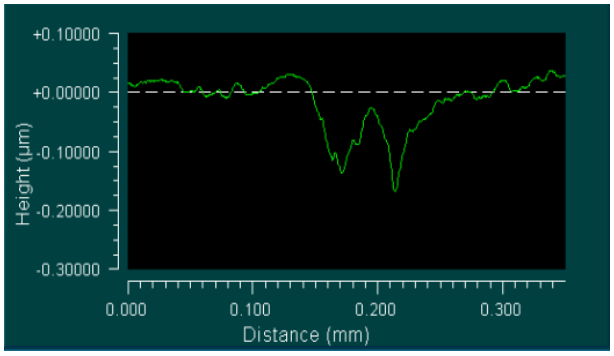

Figure 5-5 (b) Profile of cross section after tribocorrosion (1N, perpendicular to the rubbing direction).

Surfaces after tribocorrosion under mechanical rubbing with a load of 2N are shown in Figure 5-6 and Figure 5-7. Topographies of the sample surface are shown in Figure 5-6 (a) and Figure 5-7 (a). Profiles of the cross-section are shown in Figure 5-6 (b) and Figure 5-7 (b). Compared with that in Figure 5-4 (a) and Figure 5-5 (a), these pits are not round any more. As shown in Figure 5-6 (a) and Figure 5-7 (a), the sizes of the pits in the rubbing direction are bigger than the sizes in that perpendicular to the rubbing direction. The average pit length in the rubbing direction is 0.0870 mm. The

average pit length perpendicular to the rubbing direction is 0.0240 mm. As shown in Figure 5-6 (b) and Figure 5-7 (b), the depth of the pit is almost the same as that in Figure 5-4 (b) and Figure 5-5 (b). Therefore, the transformation of the pits is observed when the load is increased from 1N to 2N.

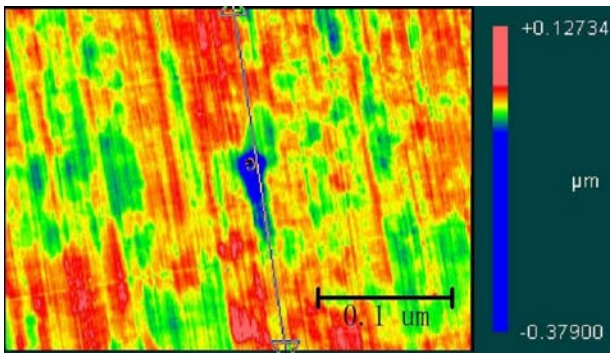

Figure 5-6 (a) Topography of surface after tribocorrosion (2N, in the rubbing direction).

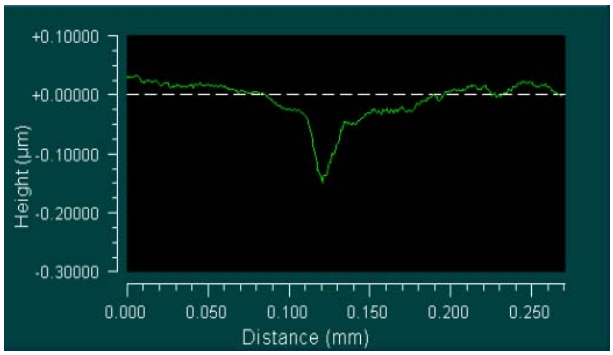

Figure 5-6 (b) Profile of cross section after tribocorrosion (2N, in the rubbing direction).

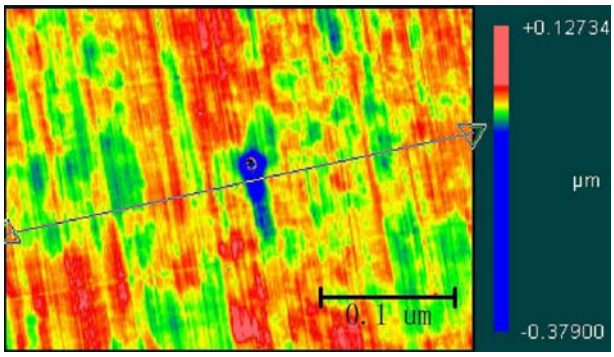

Figure 5-7 (a) Topography of surface after tribocorrosion (2N, perpendicular to the rubbing direction).

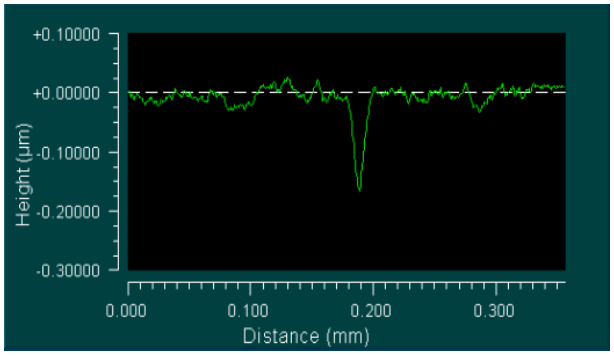

Figure 5-7 (b) Profile of cross section after tribocorrosion (2N, perpendicular to the rubbing direction).

Surfaces after tribocorrosion under mechanical rubbing with a load of 3N are shown in Figure 5-8 and Figure 5-9. Topographies of the sample surfaces are shown in Figure 5-8 (a) and Figure 5-9 (a). Profiles of cross-section are shown in Figure 5-8 (b) and Figure 5-9 (b). The transformation of the pits is more obvious under the highest load in this study. As shown in Figure 5-8 (a) and Figure 5-9 (a), the sizes of the pits in the rubbing direction are much bigger than that perpendicular to the rubbing direction. The average pit length in the rubbing direction is 0.144 mm. The average pit length

perpendicular to the rubbing direction is 0.0182 mm. The pits are more like strips. Meanwhile, as shown in Figure 5-8 (b) and Figure 5-9 (b), the pits are shallow in the cross section.

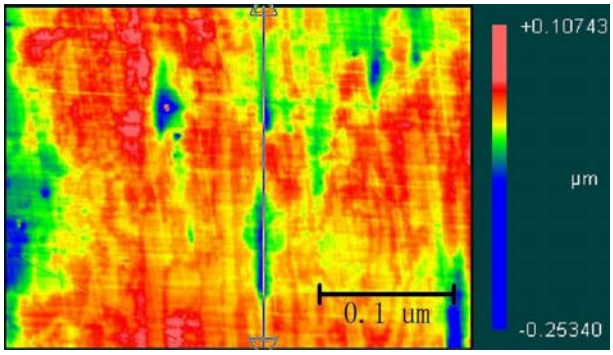

Figure 5-8 (a) Topography of surface after tribocorrosion (3N, in the rubbing direction).

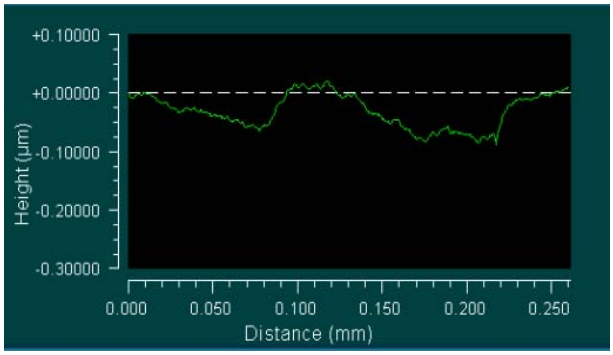

Figure 5-8 (b) Profile of cross section after tribocorrosion (3N, in the rubbing direction).

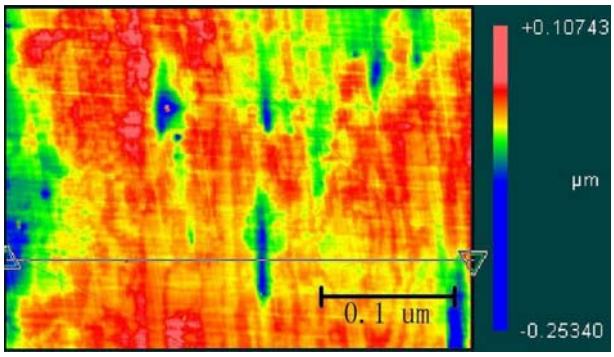

Figure 5-9 (a) Topography of surface after tribocorrosion (3N, perpendicular to the rubbing direction).

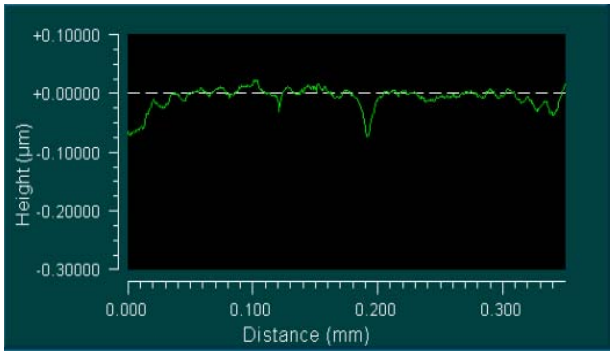

Figure 5-9 (b) Profile of cross section after tribocorrosion (3N, perpendicular to the rubbing direction).

As shown in Figure 5-10, Figure 5-11 and Figure 5-12, sizes of surface pits are concluded. The ranges and the average values of the pit sizes in rubbing direction are shown in Figure 5-10. The range and the average value of the pit size perpendicular to rubbing direction are shown in Figure 5-11. The depth of pit sizes are shown in Figure 5-12.

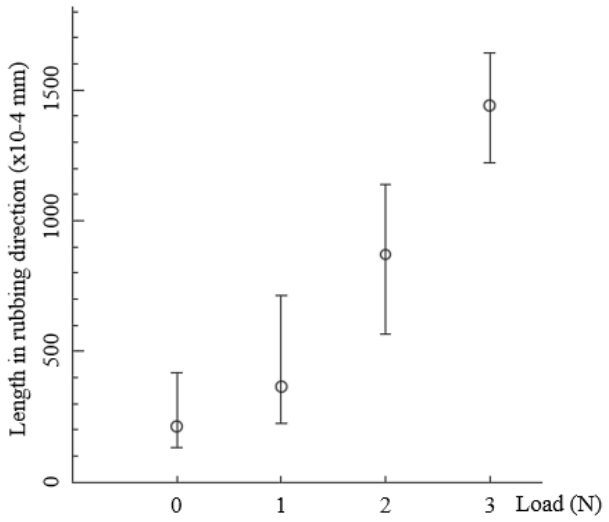

Figure 5-10 Sizes of pits in rubbing direction

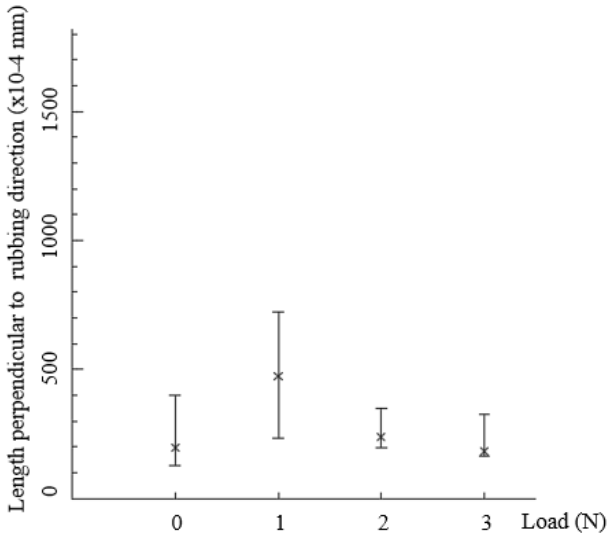

Figure 5-11 Sizes of pits perpendicular to rubbing direction

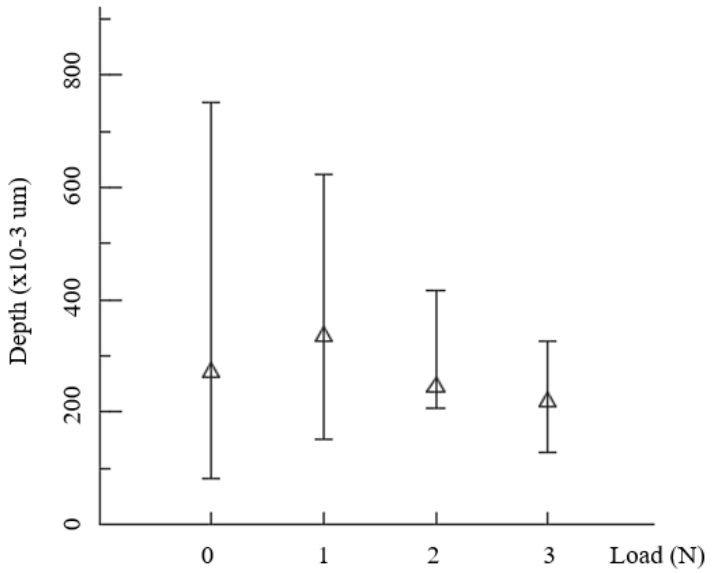

Figure 5-12 Depth of pits

As discussed above, surface characterization was conducted to study the pits after the tribocorrosion experiments. Pitting was observed in the corrosion experiments. The transformation of the pitting-like surface defects was observed after the tribocorrosion experiments under different loads. The possible mechanisms are discussed as follows. More work is needed in the future to build the detailed mechanisms.

The different tribocorrosion rate on the surface, which is caused by the different ion concentrate, is believed to be responsible for the transformation of the defects. Mechanical rubbing is believed to affect the ions distribution on the surface. As shown in Figure 5-13, in the rubbing direction, ions are forced to accumulate at two ends of the pits due to the mechanical rubbing, which causes high ion concentration in those areas. The high ion concentration causes a high tribocorrosion rate. As shown in Figure 5-14,

perpendicular to the rubbing direction, mechanical rubbing is believed to have little effect on the ion distribution. Tribocorrosion takes place relatively uniformly perpendicular to the rubbing direction. The entire ion distribution over an elongated surface pit is shown in Figure 5-15.

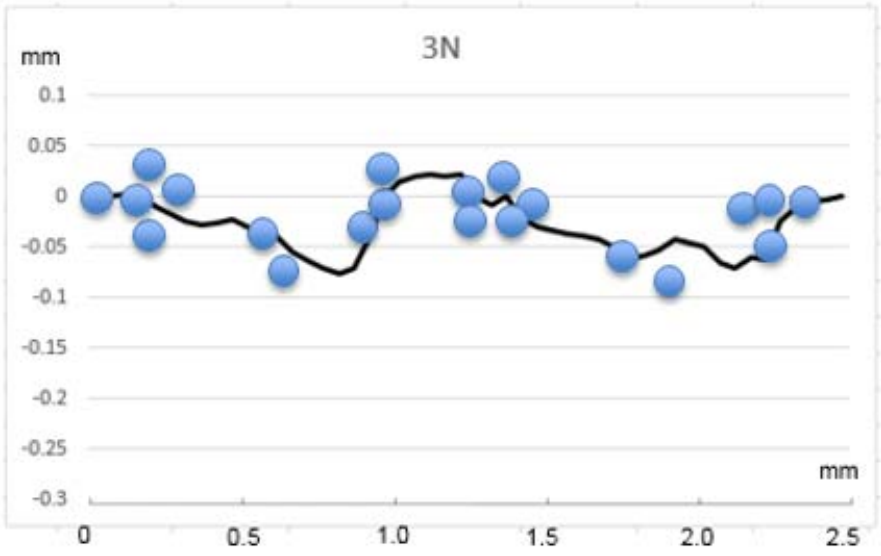

Figure 5-13 Ion distribution in the rubbing direction.

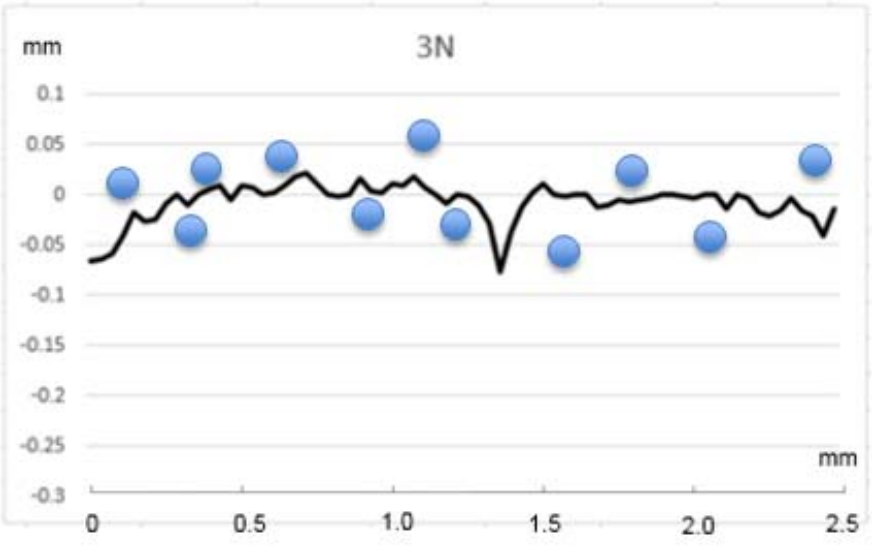

Figure 5-14 Ion distribution in that perpendicular to the rubbing direction.

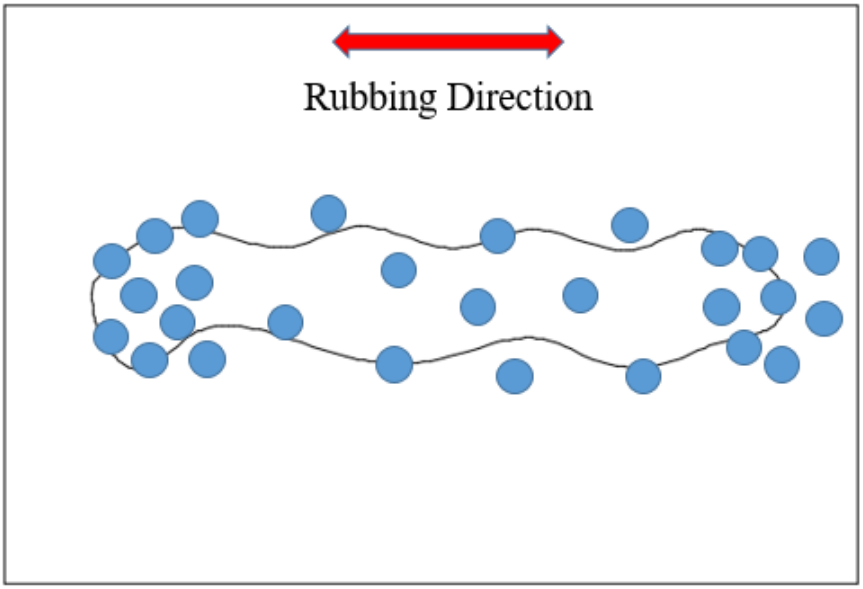

Figure 5-15 Ion distribution over an elongated surface pit

5.2 Conclusions

This section discusses about the pitting in tribocorrosion in the mild wear conditions. As discussed, pitting-like surface defects are observed in tribocorrosion. Mechanical rubbing under different loads affected pitting-like surface defects both in shapes and sizes. The possible mechanisms are also discussed.

6 CONCLUSION AND FUTURE RECOMMENDATIONS

6.1 Conclusion

This research investigated the effects of mechanical rubbing on corrosion of a duplex stainless steel 2205. It was achieved by developing an integrated triboelectrochemical approach. Through experimental design, the mild rubbing condition in the 3.5wt% salt solution was achieved. Such an approach made it possible to evaluate effects of mechanical versus chemical interactions on metal surfaces. The following highlights the major outcomes and impacts of this research.

A novel integrated triboelectrochemical approach was developed in order to study tribocorrosion in mild wear conditions. The new configuration consists a pair of flat rubbing parts, a tribometer and an electrochemical workstation. This method is superior to report because the galvanic reaction is successfully minimized. A counterpart with a larger surface area than that in the test sample was used, which ensures that mechanical rubbing is applied uniformly.

Compared with that in a conventional corrosion experiment, results in tribocorrosion showed that mechanical rubbing promoted corrosion. Meanwhile, a passivation layer was generated due to the interaction of mechanical rubbing and corrosion. When the load was increased, the passivation current density increased first then decreased. Pitting in tribocorrosion was also studied. Experimental results showed that mechanical rubbing under different loads affected the shapes and sizes of pits. After corrosion, the morphology of pits are round with an average diameter of 0.0214 mm.

Under a load of 1N, the pit-like surface defects maintain in the round shapes with an average diameter of 0.0458 mm. However, under the loads of 2N and 3N, the pits are bigger in the rubbing direction than in any other direction. Under a load of 2N, the average length in the rubbing direction of the pits is 0.0870 mm. Under a load of 3N, the average length in the rubbing direction of the pits is 0.144 mm.

6.2 Future Recommendation

In order to achieve comprehensive understanding of tribocorrosion, experiments under mild wear conditions are recommended as follows.

1. Optimization of experimental configuration

A ball joint is needed between the holder and the workpiece material in order to improve alignment and contact.

2. Identification of tribochemical reactions

The tribochemical interactions at the interface is critical for understanding tribocrorosion. The information would be useful for quantifying effects of mechanical versus chemical reactions.

3. Study of the effect of rubbing speed on tribocorrosion

A study of the role of rubbing speed is also needed. Mechanical rubbing with a higher surface speed should generate more heat, which may affect the interface reaction much more than is expected.

REFERENCES

[1] Gerhardus H.Koch, Neil G. Thompson, Y. Paul Virmani, J.H. Payer, Apr. 2015. *Corrosion Costs and Preventive Strategies in the United States*. Available from: http://www.nace.org/uploadedFiles/Publications/ccsupp.pdf.

[2] G2MT Laboratories, Apr. 2015. *Cost of Corrosion Annually in the US over $1 Trillion*. Available from: http://www.g2mtlabs.com/corrosion/cost-of-corrosion/.

[3] Giacobone, A.F.F., et al., *Microbiological induced corrosion of AA 6061 nuclear alloy in highly diluted media by Bacillus cereus RE 10.* International Biodeterioration & Biodegradation, 2011. **65**(8): p. 1161-1168.

[4] Scotto, V., et al., *Possible Chemical and Microbiological Factors Influencing Stainless-Steel Microbially Induced Corrosion (Mic) in Natural Seawater.* 5th European Congress on Biotechnology, 1990. **1**: p. 866-871.

[5] Princeton Appiled Research, May. 2015. *Application Note CORR-4: Electrochemistry and Corrosion: Overview and Techniques*. Available from: www.princetonappliedresearch.com.

[6] American Society for Testing and Materials, *G59-97*: *Standard Test Method for Conducting Potentiodynamic Polarization Resistance Measurements*.

[7] American Society for Testing and Materials, *G61-86*: *Standard Test Method for Conducting Cyclic Potentiodynamic Polarization Measurement for Localized Corrosion*.

[8] American Society for Testing and Materials, *G61-12*: *Standard Test Method for Measurement of Corrosion Potentials of Aluminum Alloys*.

[9] American Society for Testing and Materials, *G71-81*: *Standard Guide for Conducting and Evaluating Galvanic Corrosion Tests in Electrolytes*.

[10] American Society for Testing and Materials, *G82-98*: *Standard Guide for Development and Use of a Galvanic Series for Predicting Galvanic Corrosion Performce*.

[11] American Society for Testing and Materials, *G100-89*: *Standard Test Method for Conducting Cyclic Galvanostaircase Polarization*.

[12] American Society for Testing and Materials, *G150-13*: *Standard Test Method for Electrochemical Critical Pitting Temperature Testing of Stainless Steel*.

[13] Jones, D.A., *Principles and prevention of corrosion*. 1996, Upper Saddle River, NJ: Prentice Hall.

[14] American Society for Testing and Materials, *G119-09*: *Standard Guide for Determining Synergism Between Wear and Corrosion*.

[15] Kuiry, S., May. 2015. *Evaluation of Wear-Corrosion Synergy Through Tribocorrosion Studies*. Available from: https://www.bruker.com/fileadmin/user_upload/8-PDF-Docs/SurfaceAnalysis/TMT/Webinars/Evaluation_of_Wear-Corrosion_Synergy_Through_Tribocorrosion_Studies-May-2012.pdf.

[16] Vieira, A.C., et al., *Mechanical and electrochemical deterioration mechanisms in the tribocorrosion of Al alloys in NaCl and in NaNO3 solutions.* Corrosion Science, 2012. **54**: p. 26-35.

[17] von der Ohe, C.B., R. Johnsen, and N. Espallargas, *Modeling the multi-degradation mechanisms of combined tribocorrosion interacting with static and cyclic loaded surfaces of passive metals exposed to seawater.* Wear, 2010. **269**(7-8): p. 607-616.

[18] Zhang, T.C., et al., *Corrosion Wear of Duplex Stainless-Steels in Sulfuric-Acid-Solution Containing Chloride.* Corrosion, 1994. **50**(5): p. 339-344.

[19] Christian B. von der Ohe, R.J.a.N.E., 2009, *Premature Failure of Riser Tensioner Piston Rods Exposed to Offshore Splash Zone Operation – Status and Review of Critical Multi-Degradation Factors*. Available from: https://www.onepetro.org/conference-paper/NACE-09199.

[20] Archard, J., *Contact and Rubbing of Flat Surface.* Applied Physics, 1953. **24**(8): p. 981-988.

[21] Blau Peter, C.J.-P., Drees Dirk, Franek Friedrich, 2013. *Tribo-Corrosion: Research, Testing, and Applications*. 2013, Houston, TX: NACE International.

[22] Mischler, S., *Triboelectrochemical techniques and interpretation methods in tribocorrosion: A comparative evaluation.* Tribology International, 2008. **41**(7): p. 573-583.

[23] Stemp, M., S. Mischler, and D. Landolt, *The effect of contact configuration on the tribocorrosion of stainless steel in reciprocating sliding under potentiostatic control.* Corrosion Science, 2003. **45**(3): p. 625-640.

[24] Espallargas, N., et al., *A new experimental technique for quantifying the galvanic coupling effects on stainless steel during tribocorrosion under equilibrium conditions.* Wear, 2013. **307**(1-2): p. 190-197.

[25] Wood, R.J.K., *Erosion-corrosion interactions and their effect on marine and offshore materials.* Wear, 2006. **261**(9): p. 1012-1023.

[26] Gao, F. and H. Liang, *In Situ Observation of Friction-Induced Electrochemical Reactions and Impedance in Tantalum ECMP.* Journal of the Electrochemical Society, 2009. **156**(1): p. H80-H86.

[27] Gao, F. and H. Liang, *Material removal mechanisms in electrochemical-mechanical polishing of tantalum.* Electrochimica Acta, 2009. **54**(27): p. 6808-6815.

[28] Gao, F. and H. Liang, *Effects of Potential and Mechanical Stimulation on Oxidation of Tantalum During Electrochemical Mechanical Polishing.* Journal of Electronic Materials, 2012. **41**(3): p. 624-631.

[29] He, X.L., et al., *Boron-Based Nanoparticles for Chemical-Mechanical Polishing of Copper Films.* Ecs Journal of Solid State Science and Technology, 2013. **2**(1): p. P20-P25.

[30] Ng, D., et al., *Nanoparticle removal mechanisms during Post-CMP cleaning.* Electrochemical and Solid State Letters, 2007. **10**(8): p. H227-H231.

[31] Ng, D., et al., *Friction and wear-mode comparison in copper electrochemical mechanical polishing.* Journal of the Electrochemical Society, 2008. **155**(7): p. H520-H524.

[32] Joo, S. and H. Liang, *Tribo-electrochemical characterization of copper thin films.* Electrochimica Acta, 2013. **99**: p. 133-137.

[33] Kar, P., K. Wang, and H. Liang, *Force-dominated non-equilibrium oxidation kinetics of tantalum.* Electrochimica Acta, 2008. **53**(16): p. 5084-5091.

[34] J.O. Bello, R.J.K.W., J.A. Wharton, *Synergistic effects of micro-abrasion–corrosion of UNS S30403, S31603 and S32760 stainless steels.* Wear, 2007. **263**: p. 149-159.

[35] Yan, Y., et al., *Tribocorrosion in implants - assessing high carbon and low carbon Co-Cr-Mo alloys by in situ electrochemical measurements.* Tribology International, 2006. **39**(12): p. 1509-1517.

[36] Galliano, F., et al., *Tribocorrosion behavior of plasma nitrided Ti-6Al-4V alloy in neutral NaCl solution.* Surface & Coatings Technology, 2001. **145**(1-3): p. 121-131.

[37] Benea, L., et al., *Tribocorrosion behaviour of Ni-SiC nano-structured composite coatings obtained by electrodeposition.* Wear, 2009. **266**(3-4): p. 398-405.

[38] Takadoum, J., *The influence of potential on the tribocorrosion of nickel and iron in sulfuric acid solution.* Corrosion Science, 1996. **38**(4): p. 643-654.

[39] Benea, L., *Electrodeposition and tribocorrosion behaviour of ZrO2-Ni composite coatings.* Journal of Applied Electrochemistry, 2009. **39**(10): p. 1671-1681.

[40] Stojadinovic, J., et al., *Effect of electrode potential on the tribocorrosion of tungsten.* Tribology International, 2009. **42**(4): p. 575-583.

[41] Sandmeyer Steel Company, May. 2015. *Duplex/Super Duplex Stainless Steel*. Available from: http://www.sandmeyersteel.com/2205.html.

[42] University of Cambridge, Jun. 2015. *When a Metal Corrodes - the Electrical Double Layer*. Available from: http://www.doitpoms.ac.uk/tlplib/aqueous_corrosion/double_layer.php.